The genetic landscape of antibiotic sensitivity in Staphylococcus aureus

Wan Li[1,2], Menghan Liu[4,5,6], Panos Oikonomou[4,5,6], Sydney Blattman[4,5,6], Julia Hettleman[2], Joseph Gonzalez[2,], Howe Chen[2,], Saeed Tavazoie[4,5,6,7], Wenyan Jiang[1,2,3,7]

[1]These authors contributed equally
[2]Department of Genetics and Genomic Sciences, Icahn School of Medicine at Mount Sinai, New York, NY 10029, USA
[3]Department of Microbiology, Icahn School of Medicine at Mount Sinai, New York, NY 10029, USA
[4]Department of Biological Sciences, Columbia University, New York, NY 10027, USA
[5]Department of Systems Biology, Columbia University, New York, NY 10032, USA
[6]Department of Biochemistry and Molecular Biophysics, Columbia University, New York, NY 10032, USA
[7]Correspondence: wenyan.jiang@mssm.edu and st2744@columbia.edu

ABSTRACT

Despite the critical importance of essential genes, systems-level investigations of their contribution to antibiotic sensitivity have been limited. Using CRISPR Adaptation-mediated Library Manufacturing (CALM), we generated ultra-dense CRISPR interference (CRISPRi) libraries in methicillin-sensitive and -resistant strains of *Staphylococcus aureus*, which allowed us to quantify gene fitness on a global scale across ten clinically relevant antibiotics. This led to the identification of a comprehensive set of known and novel biological processes modulating bacterial fitness in the antibiotics. Notably, we found that essential genes from diverse processes dominated antibiotic-gene interactions, including a large number of synergistic interactions between bactericidal antibiotics and processes such as cell wall synthesis/cell division (CC), DNA replication/DNA recombination (DD), protein export, and coenzyme A biosynthesis. Simultaneous genetic perturbations of diverse CC and DD processes aggravated bacterial fitness, revealing a widespread synergy between the two highly coordinated processes. In contrast, perturbation of transcriptional, translational, and select energy processes antagonized the effects of bactericidal antibiotics. Finally, we show that small molecule inhibitors recapitulated synergistic antibiotic-gene interactions, providing a rational foundation for developing novel combinatorial antimicrobial therapies.

INTRODUCTION

The rise of antimicrobial resistance (AMR) is one of the biggest threats to public health. Globally, it is projected that AMR infections will cause 10 million deaths and cost US$3.5 billion annually by 2050, surpassing cancer if we do not take action[1]. Functional genomics can rapidly profile the genetic basis of diverse microbial phenotypes, including gene essentiality and antimicrobial sensitivity in bacteria, shedding lights on the rational selection of molecular targets for the development of novel antimicrobials. One such tool, transposon insertion profiling[2] and modern variations, including transposon insertion sequencing (Tn-seq)[3-7], have allowed researchers to survey the contribution of every nonessential gene to bacterial fitness in the presence of antibiotics. The application of Tn-seq to a wide range of bacterial species has revealed that genes involved in diverse biological processes, both related to and beyond the primary drug targets, can affect antibiotic sensitivity[7-11].

Antibiotics target essential bacterial pathways such as peptidoglycan synthesis, DNA replication, and protein translation. Given the central role essential genes play in bacterial physiology, we reasoned that they could be critical in modulating the killing efficacy of antibiotics. Systematic identification of essential pathways whose simultaneous inhibition aggravates bacterial fitness could lead to viable combinatorial therapeutic strategies. Drug combinations have been extensively studied and pursued in

the clinic. They have been shown to improve the efficacy of individual drugs, reduce their toxicity within hosts, and impair bacterial resistance, contributing to their therapeutic successes in infectious diseases[12-14]. Consequently, successful therapies for *Mycobacterium tuberculosis* and HIV for instance, have evolved to use drug combinations as the treatment standard. There is, thus, now a major impetus to identify more effective combinatorial antimicrobial strategies.

Despite the importance of the essential genome, systems-level efforts to delineate its contribution to antibiotic sensitivity have been lacking, partly because transposon insertion techniques exert strong, non-reversible perturbations. To address this gap, researchers have turned to the CRISPR interference (CRISPRi) technology[15,16], which mediates mild transcriptional repression rather than strong gene disruption. Recent applications of CRISPRi in bacteria by us and others have revealed novel insights into the role of essential genes in antibiotic sensitivity[17-19], showing that the genetic landscapes characterized by Tn-seq are incomplete. For instance, it was found that repression of the essential two-component system MtrAB sensitizes *M. tuberculosis* to multiple antibiotics, including rifampicin, vancomycin, and linezolid[18]. Using single- and dual-CRISPRi libraries in *Staphylococcus aureus*, we showed that repression of the essential mevalonate and fatty acid synthesis pathways enhances and diminishes, respectively, intrinsic resistance to gentamicin[19].

In this work, we performed a large-scale systems genomics study to map the landscape of antibiotic sensitivity for five bactericidal and five bacteriostatic antibiotics that target cell wall synthesis/membrane, DNA synthesis/replication, and protein translation. Facilitated by CRISPR Adaptation-mediated Library Manufacturing (CALM), a CRISPRi functional genomics platform we developed previously[19], we generated highly comprehensive genome-scale libraries in both Methicillin-sensitive *Staphylococcus aureus* (MSSA) and Methicillin-resistant *Staphylococcus aureus* (MRSA). Our study unveiled an antibiotic-gene interaction network dominated by essential genes, with synergy significantly outnumbering antagonism. Processes such as cell wall synthesis/cell division (hereafter abbreviated as CC), DNA replication/DNA recombination (hereafter abbreviated as DD), protein export, and coenzyme A biosynthesis were highly enriched for essential genes whose repression aggravated bacterial fitness in many bactericidal antibiotics. We provided direct genetic evidence supporting widespread synergistic interactions among diverse CC and DD genes. In contrast, perturbation of transcriptional, translational, and select energy processes antagonized the effects of bactericidal antibiotics, showing that inactivation of essential genes did not always promote bacterial killing. Finally, we showed that small molecule inhibitors targeting essential genes recapitulated prominent synergistic antibiotic-gene interactions discovered in our functional genomics study, laying a foundation for developing effective combinatorial antimicrobial therapies.

RESULTS

Leveraging the natural capacity of CRISPR adaptation, the CALM method we developed previously[19] can rapidly generate comprehensive genome-scale CRISPR RNA (crRNA) libraries covering 95% of all targetable sites in the *S. aureus* genome, eliminating the conventional, resource-consuming steps of guide RNA (gRNA) synthesis and cloning. Our experimental design is laid out in **Figure 1A**. First, sheared genomic DNA was electroporated into *S. aureus* cells harboring a hyperactive CRISPR-Cas adaptation machinery. This machinery functions as a “biofactory”, which manufactures genome-scale CRISPRi libraries as output. The CRISPR components necessary for transcriptional repression (ie, dCas9, crRNA and tracrRNA) are constitutively expressed. To profile the genetic landscape of antibiotic sensitivity, CRISPRi libraries generated in strains RN4220[20] and JE2[21] (which is MRSA USA300[22] cured of all its plasmids) were introduced to plain tryptic soy (TSB) media or TSB containing antibiotics targeting cell wall synthesis/membrane, DNA synthesis/replication and protein translation (**Figure 1B**). The ten antibiotics were supplied at sub-lethal concentrations (**Figure S1A**), and bacteria were grown for 9 hours, reaching early stationary phase.

The CRISPRi libraries generated by CALM were highly diverse, with close to 90% genes covered by 3 or more and the median gene covered by 10 coding-strand-targeting (CT) crRNAs (**Figure S1B**), conferring statistical robustness. We used CT crRNAs to quantify gene fitness as they mediate strong transcriptional repression[15,16]. For each crRNA, we quantified its changes of frequency in plain media and in various antibiotic conditions by $\log\frac{f_{\emptyset,9h}}{f_{\emptyset,0h}}$ and $\log\frac{f_{abx,9h}}{f_{\emptyset,9h}}$, respectively (**Figure 1A**). Next, a gene score was calculated by averaging all the CT crRNAs targeting it. Finally, we standardized the gene score by using a pool of null, intergenic crRNAs, generating a Z-score ($Z_{\emptyset}$ and Z_{abx}) that serves as the final fitness score (Methods). This standardized score allows genes from different samples to be compared across all tested antibiotic conditions – for example, a Z-score of -1 indicates a gene whose repression has a lower fitness that is one standard deviation away from the mean of the null distributed crRNAs. We found that $Z_{\emptyset}$ and Z_{abx} calculated from independent biological replicates performed on different days showed good Pearson correlations: $0.90 < r < 0.96$ for plain TSB media (**Figures S1D, E**), and $0.72 < r < 0.93$ for antibiotic conditions (**Figure S1F**).

Our CALM-CRISPR libraries showed good performance in identifying essential genes in both strains RN4220 and JE2: $0.91 < AUC < 0.95$ (**Figures S1G, H**). For instance, genes quantified with low fitness ($Z_{\emptyset}$) in TSB significantly overlapped with essential genes determined by Santiago's Tn-seq study[23] (**Figure S1K**). We found that the degree of essentiality quantified by CRISPRi varied widely for core essential biological processes, ranging from highly essential genes encoding the ribosome, RNA polymerase, tRNA ligase, and fatty acid biosynthesis, to less essential genes involved in coenzyme A biosynthesis, glycolysis, DNA recombination/DNA repair, and TCA cycle (**Figures S1L** and **S2**). For many processes such as DNA replication, cell division and peptidoglycan biosynthetic process, we observed bimodal distributions of genes with both low and high fitness. Interestingly, a similar gene differential essentiality profile was also found in *M. tuberculosis*[24]. It will be of interest to investigate the extent to which this differential essentiality is conserved at the pathway level across different bacterial species.

A large portion of essential genes modulate antibiotic sensitivity

659 out of ~2600 annotated genes in the RN4220 genome had significantly altered fitness ($|Z_{abx}| \geq 9$ and $P_{adj} < 0.05$) in at least one antibiotic condition relative to plain media, among a total of 19 conditions (including replicates) we tested (**Figure 1C**). Hierarchical clustering of these genes formed two clades. The left clade consisted of bactericidal antibiotics that target cell wall/membrane and DNA replication, which are vancomycin (vanc), daptomycin (dapt), oxacillin (oxa) and ciprofloxacin (cipro). The right clade included mostly bacteriostatic antibiotics targeting protein synthesis, with trimethoprim (tmp) and gentamicin (gent) as two exceptions. To further understand the biological function of genes modulating bacterial fitness in the antibiotics, we performed functional enrichment analysis and clustering, which identified Gene Ontology (GO) terms (**Figure 1D**) and KEGG pathways (**Figure S3A**) that were significantly overrepresented for genes with decreased and increased fitness (purple and yellow blocks, respectively). As expected, we found that inhibition of many biological processes and antibiotics with related modes of action synergized with each other. For instance, inhibition of GO terms involved in CC processes (brown labels in **Figure 1D**) reduced bacterial fitness in cell-wall/membrane-targeting antibiotics such as oxa, dapt, and vanc; inhibition of GO terms involved in DD processes (blue labels in **Figure 1D**) reduced fitness in tmp and cipro, which target nucleotide synthesis and DNA replication, respectively.

Notably, we found that essential genes dominated the antibiotic-gene interactions. Network analysis revealed that essential genes had significantly more (larger nodes) and stronger (thicker edges and shorter antibiotic-gene distances) connections with antibiotics than nonessential genes (**Figure 2A**). Indeed, perturbation of essential genes resulted in strong fitness changes ($|Z_{abx}| \geq 9$ and $P_{adj} < 0.05$) in a median of 4 antibiotic conditions, while perturbation of ~80% nonessential genes did not significantly alter fitness in any antibiotic condition (median = 0, **Figure 2B**). These results suggested that CRISPRi, with its ability to mildly perturb essential genes, delineated new genetic landscapes not attainable with

the strong loss-of function Tn-seq. Next, we found that when repressed by CRISPRi, significantly more genes aggravated bacterial fitness in bactericidal antibiotics than in bacteriostatic antibiotics under our tested conditions (P=8.3e-4, **Figure 2C**); within the bactericidal antibiotics, there were significantly more gene repression events that led to decreased fitness than to increased fitness (P=9.6e-5). This is reminiscent of a large-scale chemical genomics study in *E. coli*[25], and a comprehensive global genetic interaction (GI) network study in yeast[26], where it was found that synergistic (negative) interactions are more predominant than antagonistic (positive) interactions.

Widespread CCDD synergy

In addition to the expected synergy between antibiotics and the pathways they target, CALM-CRISPRi discovered an abundance of synergy between various CC processes and DD processes in the form of antibiotic-gene interactions. As shown in **Figure 1D**, many CC processes were significantly enriched for genes whose inhibition aggravated bacterial fitness in DNA synthesis/replication-targeting antibiotics (tmp and cipro). Similarly, inhibition of DD processes synergized with cell wall/membrane-targeting antibiotics (vanc, dapt, and oxa). To our knowledge, such widespread synergy among various CC and DD processes was not previously known, at least in *S. aureus*. For example, inhibition of a large portion of essential genes in peptidoglycan biosynthetic process (GO:0009252) and cell division (GO:0051301) significantly lowered fitness in cipro and tmp (**Figures 3A-F**). To validate these CRISPRi screening results, we cloned CT crRNAs targeting representative hit essential genes, *femX* and *ftsZ*, with an IPTG-inducible dCas9 and quantified their fitness in antibiotics. Whenever possible, we chose to validate genes that are the last in operons to avoid polar effects of CRISPRi. Bacterial fitness was quantified by pairwise competition assays performed on cloned individual crRNAs mixed with non-targeting cells as the common competitor (Methods). Of note, we chose IPTG concentrations that moderately reduced the relative fitness of candidate cells to 60-90% of that of the common competitor under no antibiotic treatment, as excessive inhibition of essential genes led to strong growth defect (or death) even without antibiotics (**Figure S4A**). Our approach confirmed that inhibition of CC processes strongly reduced fitness in oxa, dapt, vanc, cipro, and tmp (**Figures 3C** and **3F**). Similarly, inhibition of other essential processes upstream of peptidoglycan synthesis such as mevalonate pathway[27] (GO:0010142 and GO:0019287), which synthesizes the precursor to undecaprenyl phosphate, and pathways encoding cell surface glycopolymers specific to gram-positive bacteria such as teichoic acid (GO:0019350) and lipoteichoic acid (GO:0070395) biosynthetic processes[28] also reduced bacterial fitness in these antibiotics (**Figures S3B-F**). In all these examples, while the synergy between CC processes and oxa, dapt and vanc are expected, it is interesting that the CC processes also synergized with cipro, and to a lesser extent, the tmp.

Functional enrichment analysis also revealed that inhibition of various DD processes sensitized bacteria to these antibiotics (**Figure 1D**). When expression of genes encoding the two bacterial DNA homologous recombination (GO:0006310) pathways, RecFOR and RecBCD[29] (**Figure 3G**), were repressed by CRISPRi, fitness was reduced the most in the DNA replication-targeting cipro (**Figure 3H**), which was expected. Though less pronounced, fitness was also significantly reduced in antibiotics that target cell wall/membrane. For example, the fitness scores (Z_{abx}) of *addAB*, encoding the gram-positive RecBCD homologue, and those of *ruvAB*, encoding the essential Holliday junction DNA helicase, were all around -15 in oxa, dapt and vanc. In addition to DNA recombination, repression of genes encoding a number of essential proteins that constitute the DNA replication machinery (*ligA*, *polC*, *holB*, *priA*, *dnaB*), the ribonucleoside-diphosphate reductase (*nrdEF*) that converts NTPs to dNTPs, the master regulator *lexA* involved in DNA repair, and the DNA topoisomerase IV (*parEC*) as shown in **Figure 3K**, all led to reduced fitness in these three cell wall/membrane-targeting antibiotics (**Figures 3L** and **3M**). Using pairwise competition, we validated the reduced fitness for *ruvB*, *addB*, *ligA*, *nrdE*, *lexA* and *parC* in the great majority of antibiotic conditions (**Figures 3I, 3J**, and **3N-3Q**), with three conditions in *nrdE* and *parC* not reaching statistical significance. Repression of these DD genes except for *nrdE* and *parC* also showed a clear reduction in their minimum inhibitory concentration (MIC) on oxa (**Figures S4H, S4I** and **S4N-Q**). For *ruvB* and *ligA*, we also performed complementation experiments (**Figures S4R-U)**

since they precede genes of other functions in operons. We also performed CALM-CRISPRi screens in a MRSA strain, JE2, and found that repression of many of these DD genes, such as *ruvB*, *nrdE*, *priA*, *polC*, *lexA* and *parC*, significantly reduced bacterial fitness in dapt and vanc (**Figures S5C-E**), antibiotics commonly used for treating MRSA infections. Taken together, our findings show that there exists a widespread synergy among CC and DD processes, where simultaneous inhibition of CC and DD, one by antibiotic and the other by transcriptional repression, aggravated bacterial fitness. We will refer to this as the CCDD synergy.

To provide direct genetic evidence for the CCDD synergy, we created a dual-plasmid system that enables orthogonal transcriptional repression. One plasmid carried a xylose-inducible[30] antisense RNA fragment repressing a gene in CC, while the other plasmid carried an IPTG-inducible dCas9 and crRNA targeting a gene in DD (**Figure 3R**). Inducibility was necessary as all tested CCDD genes were essential. By growing cells harboring the dual-plasmid system in IPTG and xylose, we calculated the exponential phase doubling time (τ) and fitness ($1/\tau$) when CCDD genes were either not repressed, individually repressed, or simultaneously repressed (**Figure 3S**). This allowed us to quantify GI, or epistasis (ε), which measures the deviation of the actual dual perturbation effect from the expected effect based on individual perturbations. We selected five genes from CC and five genes from DD, representing ten distinct operons. With ε ranging from -1 (extreme synergy) to 1 (extreme antagonism), we found that 18 out of 25 tested CCDD interactions were synergistic ($\varepsilon < 0$ and $P < 0.05$ in **Figures 3U** and **3V**), with 9 exhibiting moderately strong synergy ($\varepsilon < -0.1$ and $P < 0.05$). To contextualize ε, we referenced data from a comprehensive yeast global GI network encompassing 90% genes[26], since such comprehensive studies have not been done in bacteria. The yeast study revealed that epistasis is generally infrequent (ie, $\varepsilon \approx 0$ for most GIs) and that $|\varepsilon| = 0.1$ represents two standard deviations from the mean of ~15 million tested GIs (**Figure 3W**). Taken together, our data indicate that the simultaneous genetic perturbation of various CC and DD genes aggravated bacterial fitness, corroborating our observed CCDD synergy in the context of antibiotic-gene interactions.

Synergy with protein export, cofactor synthesis, and fatty acid synthesis

Our functional enrichment analysis identified additional essential pathways whose inhibition strongly synergized with bactericidal antibiotics, many of which were not known previously. These included protein export, biosynthetic process of a number of organic cofactors, and fatty acid biosynthetic process (**Figures 1D and S3A**). Protein integration and transport across the membranes is an essential process ubiquitous to all domains of life. In *E. coli*, transmembrane proteins comprise approximately 25% of all cellular proteins[31]. These proteins are inserted into the membrane by the signal recognition particle (SRP) and the Sec translocation machinery and channels (**Figure 4A**). Though enrichment analysis using GO terms did not detect this biological process, likely due to over-annotation, the analysis with KEGG pathways found that inhibition of protein export (path:sao03060) synergized with CCDD-targeting bactericidal antibiotics (green labels in **Figures 1D** and **S3A**). A closer examination revealed that inhibition of a subset of the protein transport components, especially those comprising the core of SRP (4.5S RNA and Ffh) and the ATPase motor of the Sec translocation machinery (SecA), potentiated CCDD-targeting bactericidal antibiotics (**Figures 4B-D**).

Inhibition of biosynthetic process of a number of essential organic cofactors such as coenzyme A (CoA), nicotinamide adenine dinucleotide (NAD), and flavin adenine dinucleotide (FAD) also potentiated CCDD-targeting bactericidal antibiotics (**Figures 4E-M**). The coenzyme A biosynthetic process (GO:0015937) was identified by our enrichment analysis (purple label in **Figure 1D**), while neither nicotinate/nicotinamide metabolism (path:sao00760) nor riboflavin metabolism (path:sao00740) surpassed the enrichment threshold, but we found that a subset of essential genes (eg, *ppnK*, *ribF*) within these KEGG pathways significantly reduced bacterial fitness when repressed (**Figures 4I** and **4L**). CoA functions as an acyl group carrier in many biochemical reactions central to cellular metabolism[32], including fatty acid metabolism, amino acid metabolism and citric acid cycle. NAD and FAD are electron carriers equally involved in many key biochemical reactions including citric acid cycle, electron transport chains, fatty acid metabolism and DNA repair. By cloning crRNAs to target the

essential *coaA*, *ppnK*, and *ribF*, we confirmed that inhibition of biosynthesis of these cofactors aggravated bacterial fitness in CCDD-targeting bactericidal antibiotics (**Figures 4G, 4J** and **4M**), and reduced the MICs on oxa (**Figures S4E, S4K** and **S4L**).

We also identified strong synergy between processes and gent, a bactericidal antibiotic that targets the ribosome. Among those are predominantly processes involved in the nonessential ATP synthesis (GO:0046933, arrows in **Figure 1D**) and the essential fatty acid synthesis (eg, GO:0006633, maroon labels in **Figure 1D**), which corroborated the previous findings by us[19] and others[33]. A related pathway, lipid metabolic process (GO:0006629, asterisk in **Figure 1D**), contains genes involved in glycerophospholipid metabolism such as *pgsA* and *mprF* (**Figure S3G**). Our screens showed that repression of *pgsA* and *mprF* not only decreased fitness in many bactericidal antibiotics (eg, oxa, dapt, vanc and gent) that were previously shown[34-36], but also in bacteriostatic antibiotics such as erythromycin (erm), tetracycline (tet) and mupirocin (mup) (underlined in **Figure S3H**). These new findings consolidated the scientific rationale of targeting MprF as a viable antimicrobial therapeutic approach, which has been shown to strongly sensitize MRSA to dapt and nicin[37]. Collectively, our data showed that inhibition of essential genes involved in diverse biological processes aggravated bacterial fitness in bactericidal antibiotics, suggesting that combinatorial therapies may be developed by leveraging these synergistic interactions.

Antagonism

Repression of essential genes can not only synergize with but also antagonize antibiotics. We found that genes encoding the transcription (eg, GO:0000428) and translation machinery (eg, GO:0006412) were abundant among antagonistic interactions (orange and pink labels in **Figure 1D**), especially in high concentration of bactericidal antibiotics (ie, vanc 1, dapt 0.5, cipro 0.4 and gent 1) (**Figures 5A**, **5B**, **5D** and **5E**). A caveat here is that since ribosomal genes were among the most essential as quantified by our CRISPRi screens (**Figures S1L**), a large number of CT crRNAs targeting them were already dropped out even in the initial CALM-CRISPRi library at 0 hour (**Figure 1A**), due to the fact that our CRISPRi system was constitutively expressed. This resulted in many ribosomal genes containing few or no crRNAs with reliable quantification (hence P = 1 for many genes in **Figure 5E**). To address the issue of lack of quantification, we observed that the weakly repressing NCT crRNAs became useful for quantifying the fitness of highly essential genes. Unlike strong CT crRNAs, the mild NCT crRNAs were not severely dropped out in the initial library. As a result, we found that even mild repression of ribosomal genes by NCT crRNAs significantly enhanced bacterial fitness in high concentration of bactericidal antibiotics (**Figure S6A**), supplementing the incomplete data generated by CT crRNAs. Finally, we confirmed that inhibition of *rpoC* and *rplB* encoding subunits of RNA polymerase and ribosome (**Figures 5A** and **5D**), respectively, substantially increased bacterial survival in bactericidal antibiotics such as oxa, dapt, vanc and cipro (**Figures 5E** and **5F**).

Repression of a subset of genes involved in energy production, including pyruvate metabolism (path:sao00620) (arrow in **Figure S3A**) and electron transport chain (ETC) (gray labels in **Figure 1D**), also showed antagonism with many bactericidal antibiotics. Inhibition of pyruvate kinase and pyruvate dehydrogenase, enzymes located at the entrance to the TCA cycle (**Figure S6B**), enhanced bacterial survival in dapt, vanc and gent (**Figure S6C**). The staphylococcal ETC, though not comprehensively annotated, was another hit. We found that inactivation of Complex I[38] and IV significantly enhanced gent resistance (**Figure S6C**), consistent with the established body of work that disruption of the ETC reduces uptake of aminoglycosides[39]. Inactivation of Complex I also moderately enhanced bacterial survival in dapt, vanc and cipro. Altogether, these results highlight antagonism among essential processes in the context of antibiotic-gene interactions. Suppression of many essential processes including transcription, translation and energy production processes can attenuate antibiotic killing, possibly by inducing persister-like states in bacteria (see Discussion).

Antibiotic-gene synergy for bacteriostatic antibiotics

Having characterized the genetic vulnerability of bactericidal antibiotics, we next sought to investigate the vulnerability profiles for bacteriostatic antibiotics. Qualitatively, we observed that bacteriostatic antibiotics had fewer synergistic antibiotic-gene interactions than bactericidal antibiotics (**Figure 2C**). Still, we found that nuclease activity (light blue label in **Figure 1D**) was significantly enriched for genes whose repression decreased fitness in many bacteriostatic antibiotics. As underlined in **Figure 6A**, these included genes such as *rnr* involved in trans-translation[40] and *mutS2* involved in translational quality control[41]. Inactivation of these genes has been shown to reduce bacterial tolerance to protein synthesis inhibitors such as erm and lzd, which was reproduced by our MIC assays (**Figure S4V**). In addition to these two genes, we found that repression of *rnjA* (arrow in **Figure 6A**) significantly decreased bacterial fitness in all five tested bactericidal antibiotics, which was not known before. *rnjA* is classified as an essential gene by Santiago's Tn-seq study[23]. Its gene product, RNase J1, is responsible for the maturation of mRNA and 16S rRNA in *S. aureus*[42]. We confirmed our CRISPRi screening results by showing that repression of *rnjA* caused significant growth defect (**Figure 6B**) and reduced MICs in erm, lzd and mup (**Figure 6C**).

Functional genomics identifies synergistic drug combinations

One motivation of our study is to identify effective combinatorial antimicrobial strategies through functional genomics. Many genes we validated (**Figures 3** and **4**) have small molecule inhibitors (SMIs) such as visomitin (targeting RuvAB)[43], rose bengal (targeting SecA)[44] and D-pantothenol (targeting coenzyme A biosynthesis)[32]. To investigate if they can synergize with the antibiotics we tested, we performed checkerboard growth assays in various concentrations of antibiotics and SMIs. To qualify the potentiation of antibiotics by SMIs, we used two metrics – the epistasis (ε) between SMIs and antibiotics calculated by a Bliss independence model at an earlier time point when the bacteria in plain media entered stationary phase (6 hour) (**Figure 7A**), and the MIC of antibiotics measured by broth microdilution method at a terminal time point (~24 hour) (**Figure 7B**). The epistasis metric (with ε cutoff of |0.1|) was adopted from a recent large-scale drug-drug interaction study in bacteria[45]. To be stringent, we only considered a simultaneous reduction of MIC and presence of negative epistasis ($\Delta MIC \leq ½$ and $\varepsilon \leq -0.1$) to be a synergistic SMI-antibiotic interaction, as using only one metric could often be misleading (**Figures S7T** and **S7U**). Among 17 antibiotic-SMI combinations we tested on *S. aureus* RN4220, 9 resulted in synergy (**Figures 7C** and **S7A-M**). For instance, visomitin synergized with dapt and cipro, and moderately lowered their MICs by 4- and 2-fold, respectively (**Figure S7A** and **S7B**). It also lowered the MICs of gent, erm and tet by at least 4-fold (**Figures S7C-E**), consistent with our fitness validations in antibiotics (**Figure 3I**). TOFA (targeting AccABCD) strongly synergized with gent (**Figures 6F** and **S7N**), confirming the synergy between fatty acid synthesis and the antibiotic (**Figure S3I**) and is consistent with our previous finding[19]. Three SMIs, visomitin, rose bengal and TOFA, also had synergy with antibiotics in *S. aureus* USA300 (**Figures 7D** and **S7O-S**), a MRSA strain that harbors multiple resistance determinants to antibiotics including methicillin, erm, tet and mup on its chromosome and plasmids[46]. Taken together, these results demonstrated the power of CRISPRi functional genomics in identifying essential gene targets that can synergize with existing antibiotics, informing viable drug combinations for future antimicrobial therapeutics. However, we should caution that due to drug pleiotropy, drug-drug interactions may not always reflect GIs identified by functional genomics studies.

DISCUSSION

Utilizing the CALM-CRISPRi functional genomics platform, our study investigated the genetic landscape of antibiotic sensitivity in *S. aureus* across five bactericidal and five bacteriostatic antibiotics that target cell wall synthesis/membrane, DNA synthesis/replication and protein translation. This was motivated by the important roles played by essential genes in bacterial physiology and the dearth of systems-level studies of their contributions to antibiotic sensitivity. Critically, our global analyses showed that essential genes from diverse processes dominated antibiotic-gene interactions (**Figures**

2A and **2B**), a finding not manifested by previous Tn-seq studies. Contemporary CRISPRi work in *M. tuberculosis* and GI study in yeast also found that essential genes participated in significantly more antibiotic-gene[18] and gene-gene interactions[26], respectively, than nonessential genes. Moreover, all three studies revealed that synergistic interactions substantially outnumber antagonistic interactions (**Figure 2C**).

The highly sensitive CALM-CRISPRi platform and the use of both GO terms and KEGG pathways uncovered a comprehensive list of known and novel biological processes affecting bacterial fitness in antibiotics (**Figures 1D** and **S3A**). In particular, the interactions between antibiotics and many essential genes were not systematically profiled before. We found that processes such as CC, DD, protein export and various cofactor synthetic pathways were highly enriched for essential genes whose perturbation strongly aggravated bacterial fitness in bactericidal antibiotics such as oxa, dapt, vanc and cipro (**Figures 3**, **4** and **S4B-Q**). These findings could lay the foundation for developing more effective combinatorial antimicrobials. Indeed, we showed that many SMIs targeting genes in these processes synergized with existing antibiotics in both MSSA and MRSA (**Figure 7**). We also detected antagonism – perturbation of transcription, translation and energy processes significantly improved bacterial fitness in many bactericidal antibiotics (**Figures 5** and **S6**), potentially by inducing a persister-like state in bacteria. Persister bacteria are small subpopulations of phenotypic variants deficient in protein translation and metabolic activity that can survive lethal antibiotic exposure[47]. It has been shown that many bacteriostatic antibiotics targeting transcriptional and translational processes lower cellular respiration[48], which can antagonize killing by bactericidal antibiotics[49-51]. Perturbations of the TCA cycle[52] and ETC components[53] have also been shown to promote bacterial persistence. Our systems-level investigation provided the genetic basis for these phenomena, prompting more elaborately designed experiments to understand the link between the repression of select essential cellular activities and diminished antibiotic killing.

One of our key bindings was the abundant synergistic interactions between CC and DD processes, exemplified by the inhibition of CC genes and DNA replication-targeting antibiotic, cipro, as well as the inhibition of DD genes and cell wall/membrane-targeting antibiotics such as oxa, dapt and vanc (**Figures 3A-Q**). We further corroborated the antibiotic-gene synergy by genetic experiments, which showed that simultaneous repression of diverse CC and DD genes aggravated bacterial fitness (**Figure 3U**). To our knowledge, this widespread synergy between CC and DD processes has not been reported previously, though scattered evidence in other bacterial species can be found. In a small-scale (163 x ~4000) GI interaction study concentrated on nonessential genes in *E. coli*, Babu and colleagues[54] found synergistic interactions such as *ftsA-recB*, *murE-recB* and *glmSU-nrdE*. In *B. subtilis*, Peters and colleagues[55] found interactions such as *ftsL-dnaX*, *murD-dnaX* and *murC-gyrA* in an essential gene similarity network constructed based on chemical-genomic profiles. Neither study reported significantly enriched CCDD synergy, likely because their studies surveyed a relatively small nonessential GI space, or had a different focus, respectively. Interestingly, CCDD synergy is also not prominent in yeast[26]. This seems to be congruous with a fundamental difference between prokaryotes and eukaryotes: there is a temporal separation of chromosome replication (S phase) and partitioning (M phase) in eukaryotes, whereas DNA replication and cell division are highly coordinated[56-58].

Our functional genomics study provides a framework for the systematic investigation of both essential and nonessential genetic landscapes of antibiotic sensitivity, broadly applicable to diverse bacteria and environmental conditions. We are beginning to refine our understanding of how the core essential bacterial genome orchestrates cellular activities in different environments. The extensive CCDD synergy we discovered establishes a scientific rationale for a complete survey of the GIs among essential genes, or even across the entire genome, by leveraging approaches such as multiplex CRISPRi to target two genes simultaneously. We hope our study will inspire future research to explore the comprehensive GIs in diverse bacterial species, which can significantly advance our understanding of the bacterial genetic architecture and potentially lead to innovations in antimicrobial therapeutics.

ACKNOWLEDGEMENTS

We thank the Jiang lab and Tavazoie lab for insightful comments on the project. We thank Christopher D. Johnston for kindly providing the xylose-inducible plasmid, pEPSA5. This work was supported by NIH grants R00AI153530 (WJ), R01AI077562 (ST), R01GM139215 (ST) and seed fund from Icahn School of Medicine at Mount Sinai.

AUTHOR CONTRIBUTIONS

WJ conceived the study. WJ and WL performed wet-lab experiments and data analysis. SB, JH and JG assisted with cloning, DNA extraction, PCR and growth measurements. WJ performed dry-lab analysis, with assistance from ML, PO and HC. WJ and ST secured funding for the study. WJ wrote the paper.

FIGURE LEGENDS

Figure 1. Investigating the genetic landscape of antibiotic sensitivity in *Staphylococcus aureus* with CALM-CRISPRi. (**A**) Utilizing CRISPR Adaptation-mediated Library Manufacturing (CALM) technology, highly comprehensive genome-scale CRISPRi libraries can be generated in *S. aureus*. *tracr*, *hdCas9* (hyper dCas9) and R (crRNA), which are components necessary for transcriptional repression, are constitutively expressed. These libraries were subjected to outgrowth in plain TSB (∅) or sublethal concentrations of ten antibiotics (abx), followed by sequencing analysis and quantification. (**B**) The ten antibiotics used in current study. (**C**) Hierarchical clustering of 659 genes whose repression by CALM-CRISPRi significantly increased (red) or decreased (blue) bacterial fitness in at least one antibiotic condition ($|Z_{abx}| \geq 9$ and $P_{adj} < 0.05$). A total of 19 antibiotic conditions are shown. For each gene, its essentiality in plain TSB is quantified as $Z_{\varnothing}$ by CRISPRi, and qualified (binary) by previous Bae's[59] and Santiago's[23] Tn-seq studies. (**D**) Functional enrichment analysis and hierarchical clustering of significantly enriched non-redundant Gene Ontology (GO) terms. "path:sao03060 Protein export" from KEGG pathway was also included. The $\mp$log(P-value) of biological processes significantly ($P < 0.001$) enriched for genes whose repression increased and decreased fitness are shown in yellow and purple, respectively. Clustering of a full list of significant GO terms is shown in Figure S3J.

Figure 2. Essential genes dominate antibiotic-gene interactions. (**A**) Interaction networks between ten antibiotics (19 conditions) and essential genes (left), or nonessential genes (right). Antibiotics are shown as red nodes with fixed size. Genes are shown as transparent gray nodes with their size indicating the number of significant interactions with antibiotics ($|Z_{abx}| \geq 9$ and $P_{adj} < 0.05$). Synergistic and antagonistic antibiotic-gene interactions were shown as purple and brown edges, respectively, with thickness indicating Z_{abx}. (**B**) Number of antibiotic conditions in which significantly altered fitness ($|Z_{abx}| \geq 9$ and $P_{adj} < 0.05$) for Santiago's essential and nonessential genes were observed. Distributions of genes are shown as a histogram (upper) and a violin plot (lower). A Mann-Whitney U test was performed for the two gene groups. (**C**) The numbers of genes whose repression significantly decreased (blue) and increased fitness (red) ($|Z_{abx}| \geq 9$ and $P_{adj} < 0.05$) in all bactericidal antibiotics (solid circles) and bacteriostatic antibiotics (open circles) from (E). P-values from Mann-Whitney U tests are shown.

Figure 3. Widespread CCDD synergy. (**A**) Peptidoglycan biosynthetic pathway. Schematic is adapted from Jarick et al[60] with modifications. (**B**) Heatmap showing the fitness of genes in the peptidoglycan biosynthetic process (GO:0009252) in ten antibiotics as quantified by CALM-CRISPRi screens (Z_{abx}). Gene names are annotated by KEGG orthology (ko). *glmS* and *pbpA* were also added to the heatmap due to overannotation by GO terms. Genes whose repression by CRISPRi decreased and increased fitness are shown in blue and red circles, respectively. Size of circle indicates the negative of log-

transformed adjusted P-value, $-\log P_{adj}$. Gene essentiality quantified by CRISPRi (as $Z_{ø}$ in this study) and qualified (binary) by Santiago's[23] and Bae's[59] Tn-seq studies are also shown. (**C**) Pairwise competition assays measuring the fitness of *S. aureus* RN4220 carrying an IPTG-inducible CRISPRi system targeting *femX* relative to a strain carrying a non-targeting CRISPRi system in indicated antibiotic conditions (Methods). Gene of interest (*femX*) and other genes in its operon (if present) are shown in plum and pink, respectively. Concentrations of antibiotics are shown in ug/mL. Error bars indicate the standard deviation from three biological replicates. Paired t-tests were performed and * indicates $P < 0.05$. (**D**) Schematic of the divisome. (**E**) Same as (B) except heatmap is showing genes in cell division (GO:0051301). (**F**) Same as (C) except bar plot is showing the relative fitness of *ftsZ* repression. (**G**) Two homologous recombination pathways: RecFOR and AddAB. Schematic is adapted from KEGG (www.genome.jp/kegg/) with modifications. (**H**) Same as (B) except heatmap is showing genes in DNA recombination (GO:0006310). *addA*, *addB* and *recF* were also added to the heatmap due to overannotation by GO terms. (**I, J**) Same as (C) except bar plots are showing the relative fitness of *ruvB* and *addB* repression, respectively. (**K**) DNA replication pathway. Schematic is adapted from KEGG with modifications. (**L**, **M**) Same as (B) except heatmaps are showing genes in DNA replication (GO:0006260) and DNA topoisomerase activity (GO:0003916), respectively. (**N-Q**) Same as (C) except bar plots are showing the relative fitness of *ligA*, *nrdE*, *lexA* and *parC* repression, respectively. (**R**) The Two-plasmid system used to interrogate gene-gene interactions. pSpac and pXyl are IPTG- and xylose-inducible promoters driving the expression of dCas9/spacer (denoted as "S") and antisense RNA (asRNA), respectively. (**S**) Representative growth curves of cells carrying a two-plasmid system without (gray), with single (black and blue) and double (red) perturbations. Fitness (W) was calculated as the inverse of doubling time (τ) during exponentially growing phase (Methods). Epistasis between gene A and gene B ($\varepsilon_{A,B}$) is calculated as $\varepsilon_{A,B} = W_{A,B} - W_A \cdot W_B$. In this case, gene A and gene B are *ftsZ* and *lexA*, respectively. (**T**) Same as (S) except using a non-targeting two-plasmid system. (**U**) Gene-gene interaction matrix between five CC and five DD genes. For each gene-gene pair, epistasis is shown as mean of three biological replicates, normalized to the baseline of non-targeting two-plasmid system. P-values were calculated by performing a two-sample t-test between test gene-gene pairs and 27 replicates of the non-targeting two-plasmid system. (**V**) The distribution of epistasis among 25 CCDD gene pairs in (T). (**W**) To contextualize the epistasis measured in (T), we re-plotted the distribution of epistasis among ~15 million gene pairs measured in a comprehensive genetic interaction network study in yeast[26].

Figure 4. Synergy with protein export and cofactor biosynthesis. (**A**) Protein export and targeting to the membrane. Schematic is adapted from Kaushik et al[61] with modifications. Genes encoding components that strongly synergized with antibiotics are labeled in blue. (**B**) Heatmap showing the fitness of genes in the protein export (KEGG path:sao03060) pathway in ten antibiotics as quantified by CALM-CRISPRi screens (Z_{abx}). Gene names are annotated by KEGG orthology (ko). The 4.5S sRNA was also added to the heatmap. Genes whose repression by CRISPRi decreased and increased fitness are shown in blue and red circles, respectively. Size of circle indicates the negative of log-transformed adjusted P-value, $-\log P_{adj}$. Gene essentiality quantified by CRISPRi (as $Z_{ø}$ in this study) and qualified (binary) by Santiago's[23] and Bae's[59] Tn-seq studies are also shown. (**C**) Pairwise competition assays measuring the fitness of *S. aureus* RN4220 carrying an IPTG-inducible CRISPRi system targeting *secA* relative to a strain carrying a non-targeting CRISPRi system in indicated antibiotic conditions (Methods). Gene of interest (*secA*) and other genes in its operon (if present) are shown in plum and pink, respectively. Concentrations of antibiotics are shown in ug/mL. Error bars indicate the standard deviation from three biological replicates. Paired t-tests were performed and * indicates $P < 0.05$. (**D**) Same as (C) except bar plot is showing the relative fitness of *ffh* repression. (**E**) Schematic of the coenzyme A biosynthesis process. (**F**) Same as (B) except heatmap is showing genes in coenzyme A biosynthetic process (GO:0015937). (**G**) Same as (C) except bar plot is showing the relative fitness of *coaA* repression. (**H**) Schematic of nicotinate and nicotinamide metabolism. (**I**) Same as (B) except heatmap is showing genes in nicotinate and nicotinamide metabolism (KEGG path:sao00760). (**J**)

Same as (C) except bar plot is showing the relative fitness of *ppnK* repression. (**K**) Riboflavin metabolism. Riboflavin is converted to FMN and FAD by riboflavin kinase and FAD synthetase, both encoded by *ribF*. (**L**) Same as (B) except heatmap is showing genes in riboflavin metabolism (KEGG path:sao00740). (**M**) Same as (C) except bar plot is showing the relative fitness of *ribF* repression.

Figure 5. Repression of transcription and translation antagonizes bactericidal antibiotics. (**A**) The bacterial RNA polymerase complex. Schematic is adapted from KEGG (www.genome.jp/kegg/) with modifications. (**B**) Heatmap showing the fitness of genes in the DNA-directed RNA polymerase complex (GO:0000428) in ten antibiotics as quantified by CALM-CRISPRi screens (Z_{abx}). The only exception is "gent1", which shows Z_{abx} calculated from library treated with 1 ug/mL gent for 4.5 hours from a previous study[19]. Gene names are annotated by KEGG orthology (ko). Genes whose repression by CRISPRi decreased and increased fitness are shown in blue and red circles, respectively. Size of circle indicates the negative of log-transformed adjusted P-value, $-\log P_{adj}$. Gene essentiality quantified by CRISPRi (as $Z_{ø}$ in this study) and qualified (binary) by Santiago's[23] and Bae's[59] Tn-seq studies are also shown. Genes labeled with "NCT" indicate that due to extreme gene essentiality, quantification of Z_{abx} had to be performed using NCT crRNAs. However, $Z_{ø}$ was still quantified using CT crRNAs. (**C**) Pairwise competition assays measuring the fitness of *S. aureus* RN4220 carrying an IPTG-inducible CRISPRi system targeting *rpoC* relative to a strain carrying a non-targeting CRISPRi system in indicated antibiotic conditions (Methods). Gene of interest (*rpoC*) and other genes in its operon (if present) are shown in plum and pink, respectively. Concentrations of antibiotics are shown in ug/mL. Error bars indicate the standard deviation from three biological replicates. Paired t-tests were performed and * indicates $P < 0.05$. (**D**) The bacterial ribosome. Schematic is adapted from KEGG with modifications. (**E**) Same as (B) except heatmap is showing genes in ribosome (GO:0005840). (**F**) Same as (C) except bar plot is showing the relative fitness of *rplB* repression.

Figure 6. Select nuclease activity affects fitness in bacteriostatic antibiotics. (**A**) Heatmap showing the fitness of genes in the nuclease activity (GO:0004518) in ten antibiotics as quantified by CALM-CRISPRi screens (Z_{abx}). Gene names are annotated by KEGG orthology (ko). Genes whose repression by CRISPRi decreased and increased fitness are shown in blue and red circles, respectively. Size of circle indicates the negative of log-transformed adjusted P-value, $-\log P_{adj}$. Gene essentiality quantified by CRISPRi (as $Z_{ø}$ in this study) and qualified (binary) by Santiago's[23] and Bae's[59] Tn-seq studies are also shown. (**B**) *S. aureus* RN4220 carrying an IPTG-inducible CRISPRi system targeting *rnjA* or a non-targeting CRISPRi system grown on TSA with varying concentrations of IPTG at 37 °C for 24 hours. (**C**) Upper: *rnjA* and other genes in its operon are shown in plum and pink, respectively. Lower: checkerboard assays to test the MICs of erm, lzd and mup. *S. aureus* RN4220 carrying an IPTG-inducible CRISPRi system targeting *rnjA* or a non-targeting CRISPRi system were spotted on TSA plates containing varying concentrations of antibiotics (x-axis) and IPTG (y-axis). Approximately 50 – 100 CFUs were spotted on these plates and grown for 48 hours at 37 °C.

Figure 7. Synergistic drug combinations. (**A**) A representative checkerboard growth assay of vancomycin-RB combination for *S. aureus* RN4220. Checkerboard shows normalized bacterial growth (to the bottom left well containing plain TSB) in various concentrations of antibiotic and SMI at 6 hours post inoculation when bacteria in plain TSB entered stationary phase. Epistasis (ε) was calculated for the well corresponding to (RB 0.5 and vanc 1). Concentrations of SMI and antibiotic are in ug/mL. (**B**) Same as (A) except showing normalized bacterial growth at 24 hours post inoculation. Change of MIC is shown. (**C**) Interactions between antibiotics (x-axis) and SMIs (y-axis) in *S. aureus* RN4220 quantified by checkerboard assays. Targets of SMIs are shown in parentheses. Epistasis (ε) and change in MIC (ΔMIC) were quantified. 9 out of 17 tested combinations were considered synergistic (ΔMIC ≤ ½ and ε ≤ -0.1). (**D**) Same as (C) except showing antibiotic-SMI interactions in *S. aureus* USA300.

Materials and Methods

Bacterial strains and Culture Conditions

Cultivation of *Staphylococcus aureus* strains RN4220[20], USA300[22], JE2[21] were carried out in tryptic soy broth (TSB) medium (BD) at 37 °C with shaking (rpm 220), or tryptic soy agar (TSA) plates. Whenever necessary, medium was supplemented with appropriate antibiotics to select for plasmid transformation. In these cases, the concentrations of antibiotics were as follows: chloramphenicol, 10 µg/mL; erythromycin, 10 µg/mL; tetracycline, 5 µg/mL.

Cloning

Plasmid pWJ584 was constructed by Gibson assembly of two PCR products. One PCR was performed using plasmid pWJ402 and primers W1956 and W1948. Another PCR was performed using pWJ420 and primers W1957 and W1961.

Plasmid pWJ587 was constructed by Gibson assembly of two PCR products. One PCR was performed using plasmid pWJ418 and primers W1341 and W1342. Another PCR was performed using pWJ444 and primers W1971 and W1972.

Similar to previous studies[16,19], CRISPR spacer cloning was performed by ligation of annealed oligonucleotide pairs and BsaI-digested parent vector, pWJ444 (constitutive dCas9) or pWJ587 (IPTG-inducible dCas9). Plasmids pWJ402, pWJ418, pWJ420, pWJ444 were previously published[19].

Antisense RNA fragments were cloned to plasmid pEPSA5 containing a xylose-inducible promoter.

All PCRs and Gibson assembly reactions were performed using Q5® High-Fidelity DNA Polymerase and NEBuilder® HiFi DNA Assembly Master Mix supplied by NEB, respectively.

Checkerboard assays for measuring MIC

A single colony (10^6-10^7 CFUs) of *S. aureus* RN4220 cells carrying a chloramphenicol-resistant plasmid encoding IPTG-inducible dCas9 and a spacer targeting gene of interest was re-suspended in 100 µL 1X PBS. Serial dilutions of the re-suspended cells were spotted on 5 x 4 TSA plates containing 5 µg/mL chloramphenicol (to keep CRISPRi plasmid targeting genes of interest) and various concentrations of IPTG and testing antibiotics. The checkerboard format was necessary as a range of IPTG concentrations was necessary to capture the optimal transcriptional repression levels for different essential genes. Typically, TSA was supplemented with following IPTG concentrations: 0.003, 0.01, 0.03, 0.1 and 0.3 mM.

Checkerboard assays for antibiotic-SMI interactions

Synergy H1 microplate reader (Biotek) was used to perform checkerboard assays. Typically, Corning™ 3370 Clear Polystyrene 96-Well Microplates were used to harbor a 7 x 7 checkerboard containing 200 µL TSB with varying concentrations of antibiotics and SMIs. 5 – 10 single colonies of *S. aureus* RN4220 or USA300 cells was re-suspended in 200 µL 1X PBS. 2 µL of re-suspended cells were inoculated into 200 µL media in each well of checkerboard. Microplates were grown at 37°C with shaking (548 cpm) for 20 – 24 h. The absorbance at 600nm (OD_{600}) was measured every 10 minutes.

Gene-gene interaction measurement

To measure epistasis between CC and DD genes, *S. aureus* RN4220 carrying dual-plasmid systems were cloned. A chloramphenicol-resistant plasmid driving a xylose-inducible antisense RNA fragment was used to repress CC genes. Another tetracycline-resistant plasmid driving an IPTG-inducible dCas9 and crRNA was used to repress DD genes. For each CCDD combination, 5 – 10 single colonies of *S. aureus* RN4220 carrying dual-plasmid systems was re-suspended in 200 µL 1X PBS. 2 µL of re-suspended cells were inoculated into 200 µL TSB containing 5 µg/mL chloramphenicol, 2.5 µg/mL tetracycline, as well as xylose and IPTG concentrations that were empirically determined. This means repression of the essential CC and DD genes was induced at time 0. Cultures were grown in

Synergy H1 microplate reader at 37°C with shaking (548 cpm) for up to 16 h. The absorbance at 600nm (OD_{600}) was measured every 10 minutes. We calculated the average doubling time (τ) between OD_{600} of 0.125 and 0.5 for cells without, with single and double perturbations. To do so, a linear regression on growth data for which the $\log_2$ of blanked OD_{600} was between 0.125 and 0.5 was used. The rationale for choosing this OD_{600} range was that cells were in exponentially growing phase, and sufficient time had elapsed (~4 h) for the induction of repression of CC and DD genes. Next, fitness (W) was calculated as 1/τ. Triplicates were performed for each CCDD combination. Genetic interaction between gene A and gene B, or epistasis (ε), was calculated as $\varepsilon_{A,B} = W_{A,B} - W_A \cdot W_B$. As controls, 27 replicates were also performed on a non-targeting two-plasmid system (ie, parental plasmids that were not cloned with CC and DD targets) in the presence of xylose and IPTG. Accordingly, the baseline epistasis can be calculated as $\varepsilon_{Ø1,Ø2} = W_{Ø1.Ø2} - W_{Ø1} \cdot W_{Ø2}$. The interaction for each CCDD combination was than normalized by $\varepsilon_{A,B\,(norm)} = \varepsilon_{A,B} - \varepsilon_{Ø1,Ø2}$, which was shown in the matrix in **Figure 3S**. P-value for each interaction was calculated by performing a two-sample t-test between triplicates of $\varepsilon_{A,B}$ and 27 replicates of $\varepsilon_{Ø1,Ø2}$.

Using CALM-CRISPRi to measure gene fitness in plain TSB and antibiotics

Method for generating genome-scale CRISPRi libraries in *S. aureus* is similar to our previous study[19]. The CALM-CRISPRi machinery is encoded on a single plasmid, pWJ584, which contains *tracr*, hd*cas9*, an empty CRISPR array (denoted as "R"), *cas1*, *cas2*, *csn2* (**Figure 1A**) and a chloramphenicol-resistant cassette. The CRISPR adaptation machinery (*cas1*, *cas2* and *csn2*) is under an IPTG-inducible promoter, pSpac). CRISPR components necessary for transcriptional repression (ie, hdCas9, crRNA and tracrRNA) are constitutively expressed. To start, a single colony of *S. aureus* RN4220 or JE2 strains harboring pWJ584 was grown overnight in 4 mL of TSB with chloramphenicol (5 µg/mL). Culture was diluted 1:200 in 15 mL of fresh TSB (no antibiotics) with 2 mM IPTG to induce the expression of Cas1, Cas2 and Csn2 and grown until OD_{600} reached 1.0 (typically 3 – 4 h). To make competent cells, cells were pelleted and washed two times using one volume of sterile water at room temperature. Cells were ultimately re-suspended in 1/100th volume of sterile water. It is crucial to perform these steps at room temperature and avoid cold shocking bacterial cells, as we observed that cells prepared at 4 °C contained libraries with considerably more spacers matching the plasmid rather than the chromosome.

50 µL of competent cells were mixed with 2 µg of sheared genomic DNA (to an average of 150 bp) prepared from the same host and incubated 5 min at room temperature. Electroporation was performed using MicroPulser (Bio-Rad) with the default staph program (2 mm, 1.8 kV and 2.5 ms). Of note, we found ~50% of the cells were killed by electroporation, which was moderate. After electroporation, cells were immediately re-suspended in 500 µL of TSB and recovered at 37 °C for 15 min with shaking. Next, 200 µL of recovered cells were transferred to 15 mL of pre-warmed TSB with chloramphenicol (5 µg/mL) and recovered for an additional 5 h at 37 °C with shaking. During this recovery period, CRISPR adaptation occurred, and the resulting culture, typically at OD_{600} = 3.0 or 10^9 CFU/mL, constituted the genome-scale CRISPRi library we deemed as Time 0 h in **Figure 1A**. Typically, 7 mL of the library culture was pelleted, lysed, amplified by PCR and sent for Illumina sequencing.

To profile the genetic fitness landscape of *S. aureus* in antibiotics, 7 mL of CALM-CRISPRi library were transferred to a 2L Erlenmeyer flask containing 700 mL of plain TSB (pre-warmed at 37 °C), or TSB containing sublethal concentrations of tested antibiotics, including oxacillin (0.05 µg/mL), daptomycin (0.25 and 0.5 µg/mL), vancomycin (1 µg/mL), ciprofloxacin (0.2 and 0.4 µg/mL), gentamicin (0.5 µg/mL), trimethoprim (0.4 µg/mL), erythromycin (0.08 µg/mL), tetracycline (0.04 µg/mL), linezolid (0.2 and 0.25 µg/mL), and mupirocin (0.02 µg/mL). Chloramphenicol was not added during this selection to avoid potential drug-drug interactions. Whenever daptomycin was used, media was also supplemented with 1 mM $CaCl_2$. Cultures were incubated at 37 °C, 140 rpm for 9 hours, reaching 4 – 5 in OD_{600}. Finally, 7 mL of the culture was pelleted, lysed, amplified by PCR and sent for Illumina sequencing.

Pairwise competition assay

S. aureus RN4220 cells harboring an inducible dCas9, along with no spacer (pWJ587) and spacers targeting genes of interest were cloned. All spacers were cloned into the pWJ587 backbone with a chloramphenicol-resistant (cm^R) marker.

Pairwise competition assay[62,63] was performed to calculate the fitness of RN4220 carrying spacers targeting genes of interest, relative to RN4220 carrying no spacer (ie, pWJ587), which acted as the common competitor. First, RN4220 with spacer targeting the gene of interest (candidate) and the common competitor were streaked on TSA plates supplemented with 5 µg/mL chloramphenicol and incubated at 37°C for 14 – 20 hours. Equal amount of candidate the common competitor were mixed by picking and re-suspending single colonies in 1X PBS to an OD_{600} of 0.1 measured by plate reader. 2 uL of mixed bacteria were inoculated into 200 uL TSB containing IPTG and appropriate antibiotics whenever necessary. Microplates were grown at 37 °C with shaking (548 cpm) for 20 – 24 h. After growth, 150 uL of bacteria in each condition were transferred to an 1.5 mL Eppendorf tube, pelleted and washed with 1X PBS. Importantly, as candidate genes were essential, it was necessary to choose IPTG concentrations that reduced the fitness of these genes by 60-90% relative to that of the common competitor under no antibiotic treatment.

To quantify the ratio of candidate and common competitor, pelleted cells were lysed, minipreped, and subjected to PCR. For each PCR, a 20 uL reaction mixed was prepared by adding approximately 20 ng plasmid DNA as template, 0.2 uM of forward primer (W1201), 0.2 uM of reverse primers (L401) and One*Taq*® DNA polymerase (NEB). DNA bands were visualized on 2% agarose gel containing ethidium bromide. Intensity of DNA bands corresponding to spacers of interest (211 bp) and the common competitor (empty array, 145 bp) were quantified by ImageJ. An example of *ftsZ* is shown in **Figure S1J**. At the beginning and end of pairwise competition assay, we also spotted bacteria on TSA plates containing 5 µg/mL chloramphenicol and incubated at 37°C for 14 – 20 hours. Combined with the ratios obtained from PCR, it allowed us determine the initial and final population size of the candidate and the common competitor. Thus, fitness of candidate strain with spacer targeting gene *X* (W_X) was calculated as relative to that of the common competitor:

$$W_X = \frac{\ln\left(\frac{N_{X,f}}{N_{X,i}}\right)}{\ln\left(\frac{N_{C,f}}{N_{C,i}}\right)}$$

where N_X and N_C are the population sizes of gene *X* strain and the common competitor, and subscripts *f* and *i* indicate the final and initial time points, respectively.

Sequencing analysis and gene fitness quantification

In this study, we quantified gene fitness in plain TSB ($Z_ø$) and in antibiotics (Z_{abx}). The detailed steps for quantification are described below.

For each crRNA, the normalized frequency of it, $f_{\text{sample}}^{\text{crRNA}}$, is calculated by dividing its reads by the total number of reads in that sample. The fitness of each crRNA in plain TSB media (Ø) is calculated as the log2-transformed fold-change of frequency of crRNA measured at 9 hour to that measured at 0 hour:

$$\log_2 \text{FC}_{ø}^{\text{crRNA}} = \log_2 \frac{f_{ø,9\text{h}}^{\text{crRNA}}}{f_{ø,0\text{h}}^{\text{crRNA}}}$$

For each gene, we quantify $\log_2 \mathrm{FC}_{\emptyset}^{\mathrm{gene}}$ by averaging all CT crRNAs targeting that gene. To minimize potential off-target effect, we ranked all $\log_2 \mathrm{FC}_{\emptyset}^{\mathrm{crRNA}}$ s in ascending orders (ie, from $\log_2 \mathrm{FC}_{\emptyset}^{\mathrm{crRNA}_1}$ to $\log_2 \mathrm{FC}_{\emptyset}^{\mathrm{crRNA}_n}$) and removed the CT crRNAs with the lowest and the highest values, unless the gene has three or fewer CT crRNAs. This gives:

$$\log_2 \mathrm{FC}_{\emptyset}^{\mathrm{gene}} = \frac{\log_2 \mathrm{FC}_{\emptyset}^{\mathrm{crRNA}_2} + \log_2 \mathrm{FC}_{\emptyset}^{\mathrm{crRNA}_3} + \cdots + \log_2 \mathrm{FC}_{\emptyset}^{\mathrm{crRNA}_{n-1}}}{n-2}$$

Subsequently, $\log_2 \mathrm{FC}_{\emptyset}^{\mathrm{gene}}$ was standardized by Z-scoring, using pseudogenes made up by null crRNAs. As our CALM-CRISPRi platform routinely generated highly comprehensive crRNA libraries covering ~95% of all targetable sites in the genome, encompassing diverse genetic elements and intergenic regions, we assigned ~4,000 crRNAs targeting chromosomal intergenic regions as null crRNAs (**Figure S1I**). For each treatment condition, fifty random null crRNAs were chosen from them to create a pseudogene, and fitness of the pseudogene, $\log_2 \mathrm{FC}_{\emptyset}^{\mathrm{pseudo}}$, was calculated by averaging these null crRNAs. Next, a collection of one hundred pseudogenes were created in this manner, and the mean and standard deviation of one hundred $\log_2 \mathrm{FC}_{\emptyset}^{\mathrm{pseudo}}$s were calculated as $< \log_2 \mathrm{FC}_{\emptyset}^{\mathrm{pseudo}} >$ and $\sigma_{\emptyset}^{\mathrm{pseudo}}$, respectively. This allowed us to calculate Z-scores for each gene:

$$\mathbf{Z}_{\emptyset}^{\mathbf{gene}} = \frac{\log_2 \mathrm{FC}_{\emptyset}^{\mathrm{gene}} - < \log_2 \mathrm{FC}_{\emptyset}^{\mathrm{pseudo}} >}{\sigma_{\emptyset}^{\mathrm{pseudo}}}$$

This standardized Z-score, serving as the final gene fitness score, allows samples to be comparable across all tested conditions, including plain TSB media (Ø) and antibiotic treatments (abx).

Similarly, gene fitness can be also quantified in antibiotic conditions, as shown below:

$$\log_2 \mathrm{FC}_{\mathrm{abx}}^{\mathrm{crRNA}} = \log_2 \frac{f_{\mathrm{abx,9h}}^{\mathrm{crRNA}}}{f_{\emptyset,\mathrm{9h}}^{\mathrm{crRNA}}}$$

$$\log_2 \mathrm{FC}_{\mathrm{abx}}^{\mathrm{gene}} = \frac{\log_2 \mathrm{FC}_{\mathrm{abx}}^{\mathrm{crRNA}_2} + \log_2 \mathrm{FC}_{\mathrm{abx}}^{\mathrm{crRNA}_3} + \cdots + \log_2 \mathrm{FC}_{\mathrm{abx}}^{\mathrm{crRNA}_{n-1}}}{n-2}$$

$$\mathbf{Z}_{\mathbf{abx}}^{\mathbf{gene}} = \frac{\log_2 \mathrm{FC}_{\mathrm{abx}}^{\mathrm{gene}} - < \log_2 \mathrm{FC}_{\mathrm{abx}}^{\mathrm{pseudo}} >}{\sigma_{\mathrm{abx}}^{\mathrm{pseudo}}}$$

For each gene, a Mann-Whitney U test was used to determine if the fitness of all CT crRNAs targeting it significantly deviates from null crRNAs of the pseudogenes. The resulting P-value is adjusted by the Benjamini-Hochberg method.

Throughout, $\mathrm{Z}_{\emptyset}^{\mathrm{gene}}$ and $\mathrm{Z}_{\mathrm{abx}}^{\mathrm{gene}}$ have been simplified as $Z_{\emptyset}$ and Z_{abx}, respectively.

We also quantified gene fitness using the mildly-targeting NCT crRNAs, which are useful when quantifying highly essential genes such as those involved in ribosome, RNA polymerase, and fatty acid synthesis. The general flow of quantification is the same as before except that NCT, instead of CT crRNAs were used for each gene.

$$\log_2 \mathrm{FC}_{\mathrm{abx}}^{\mathrm{NCT\ crRNA}} = \log_2 \frac{f_{\mathrm{abx,9h}}^{\mathrm{NCT\ crRNA}}}{f_{\emptyset,\mathrm{9h}}^{\mathrm{NCT\ crRNA}}}$$

$$\log_2 \mathrm{FC}_{\mathrm{abx}}^{\mathrm{gene(NCT)}} = \frac{\log_2 \mathrm{FC}_{\mathrm{abx}}^{\mathrm{NCT\ crRNA_2}} + \log_2 \mathrm{FC}_{\mathrm{abx}}^{\mathrm{NCT\ crRNA_3}} + \cdots + \log_2 \mathrm{FC}_{\mathrm{abx}}^{\mathrm{NCT\ crRNA}_{n-1}}}{n-2}$$

$$\mathrm{Z}_{\mathrm{abx}}^{\mathrm{gene\ (NCT)}} = \frac{\log_2 \mathrm{FC}_{\mathrm{abx}}^{\mathrm{gene\ (NCT)}} - < \log_2 \mathrm{FC}_{\mathrm{abx}}^{\mathrm{pseudo}} >}{\sigma_{\mathrm{abx}}^{\mathrm{pseudo}}}$$

Functional enrichment analysis

Functional enrichment analysis was performed using iPAGE, an information-theoretic pathway analysis tool[64] we previously developed. We used both KEGG pathway (https://www.genome.jp/kegg-bin/show_organism?menu_type=pathway_maps&org=sao) and GO term annotations (https://biocyc.org/GCF_000013425/organism-summary) for *S. aureus* NCTC 8325, a parental strain for RN4220. Overall, ~37% and ~83% of the RN4220 genome is annotated by KEGG pathways and GO terms, respectively. While KEGG pathways are poorly annotated in *S. aureus* (eg, well known genes such as *ftsZ*, *lexA*, *addAB* have no annotated pathways), GO terms tend to over-annotate, which can also lead to dilution of significant pathways.

References

1 O'Neill, J. Tackling drug-resistant infections globally: final report and recommendations. *Review on Antimicrobial Resistance* (2016).

2 Girgis, H. S., Liu, Y., Ryu, W. S. & Tavazoie, S. A comprehensive genetic characterization of bacterial motility. *PLoS genetics* **3**, 1644-1660, doi:10.1371/journal.pgen.0030154 (2007).

3 van Opijnen, T., Bodi, K. L. & Camilli, A. Tn-seq: high-throughput parallel sequencing for fitness and genetic interaction studies in microorganisms. *Nature methods* **6**, 767-772, doi:10.1038/nmeth.1377 (2009).

4 Langridge, G. C. *et al.* Simultaneous assay of every Salmonella Typhi gene using one million transposon mutants. *Genome research* **19**, 2308-2316, doi:10.1101/gr.097097.109 (2009).

5 Goodman, A. L. *et al.* Identifying genetic determinants needed to establish a human gut symbiont in its habitat. *Cell host & microbe* **6**, 279-289, doi:10.1016/j.chom.2009.08.003 (2009).

6 Gawronski, J. D., Wong, S. M., Giannoukos, G., Ward, D. V. & Akerley, B. J. Tracking insertion mutants within libraries by deep sequencing and a genome-wide screen for Haemophilus genes required in the lung. *Proceedings of the National Academy of Sciences of the United States of America* **106**, 16422-16427, doi:10.1073/pnas.0906627106 (2009).

7 Girgis, H. S., Hottes, A. K. & Tavazoie, S. Genetic architecture of intrinsic antibiotic susceptibility. *PloS one* **4**, e5629, doi:10.1371/journal.pone.0005629 (2009).

8 Xu, W. *et al.* Chemical Genetic Interaction Profiling Reveals Determinants of Intrinsic Antibiotic Resistance in Mycobacterium tuberculosis. *Antimicrobial agents and chemotherapy* **61**, doi:10.1128/AAC.01334-17 (2017).

9 Rajagopal, M. *et al.* Multidrug Intrinsic Resistance Factors in Staphylococcus aureus Identified by Profiling Fitness within High-Diversity Transposon Libraries. *mBio* **7**, doi:10.1128/mBio.00950-16 (2016).

10 Leshchiner, D. *et al.* A genome-wide atlas of antibiotic susceptibility targets and pathways to tolerance. *Nature communications* **13**, 3165, doi:10.1038/s41467-022-30967-4 (2022).

11 Murray, J. L., Kwon, T., Marcotte, E. M. & Whiteley, M. Intrinsic Antimicrobial Resistance Determinants in the Superbug Pseudomonas aeruginosa. *mBio* **6**, e01603-01615, doi:10.1128/mBio.01603-15 (2015).

12 Silver, L. L. Challenges of antibacterial discovery. *Clinical microbiology reviews* **24**, 71-109, doi:10.1128/CMR.00030-10 (2011).

13 Tyers, M. & Wright, G. D. Drug combinations: a strategy to extend the life of antibiotics in the 21st century. *Nature reviews. Microbiology* **17**, 141-155, doi:10.1038/s41579-018-0141-x (2019).
14 Gray, D. A. & Wenzel, M. Multitarget Approaches against Multiresistant Superbugs. *ACS infectious diseases* **6**, 1346-1365, doi:10.1021/acsinfecdis.0c00001 (2020).
15 Qi, L. S. *et al.* Repurposing CRISPR as an RNA-guided platform for sequence-specific control of gene expression. *Cell* **152**, 1173-1183, doi:10.1016/j.cell.2013.02.022 (2013).
16 Bikard, D. *et al.* Programmable repression and activation of bacterial gene expression using an engineered CRISPR-Cas system. *Nucleic acids research* **41**, 7429-7437, doi:10.1093/nar/gkt520 (2013).
17 Ward, R. D. *et al.* Essential gene knockdowns reveal genetic vulnerabilities and antibiotic sensitivities in Acinetobacter baumannii. *mBio* **15**, e0205123, doi:10.1128/mbio.02051-23 (2024).
18 Li, S. *et al.* CRISPRi chemical genetics and comparative genomics identify genes mediating drug potency in Mycobacterium tuberculosis. *Nature microbiology* **7**, 766-779, doi:10.1038/s41564-022-01130-y (2022).
19 Jiang, W., Oikonomou, P. & Tavazoie, S. Comprehensive Genome-wide Perturbations via CRISPR Adaptation Reveal Complex Genetics of Antibiotic Sensitivity. *Cell* **180**, 1002-1017 e1031, doi:10.1016/j.cell.2020.02.007 (2020).
20 Nair, D. *et al.* Whole-genome sequencing of Staphylococcus aureus strain RN4220, a key laboratory strain used in virulence research, identifies mutations that affect not only virulence factors but also the fitness of the strain. *Journal of bacteriology* **193**, 2332-2335, doi:10.1128/JB.00027-11 (2011).
21 Fey, P. D. *et al.* A genetic resource for rapid and comprehensive phenotype screening of nonessential Staphylococcus aureus genes. *mBio* **4**, e00537-00512, doi:10.1128/mBio.00537-12 (2013).
22 Kennedy, A. D. *et al.* Epidemic community-associated methicillin-resistant Staphylococcus aureus: recent clonal expansion and diversification. *Proceedings of the National Academy of Sciences of the United States of America* **105**, 1327-1332, doi:10.1073/pnas.0710217105 (2008).
23 Santiago, M. *et al.* A new platform for ultra-high density Staphylococcus aureus transposon libraries. *BMC genomics* **16**, 252, doi:10.1186/s12864-015-1361-3 (2015).
24 Bosch, B. *et al.* Genome-wide gene expression tuning reveals diverse vulnerabilities of M. tuberculosis. *Cell* **184**, 4579-4592 e4524, doi:10.1016/j.cell.2021.06.033 (2021).
25 Nichols, R. J. *et al.* Phenotypic landscape of a bacterial cell. *Cell* **144**, 143-156, doi:10.1016/j.cell.2010.11.052 (2011).
26 Costanzo, M. *et al.* A global genetic interaction network maps a wiring diagram of cellular function. *Science* **353**, doi:10.1126/science.aaf1420 (2016).
27 Balibar, C. J., Shen, X. & Tao, J. The mevalonate pathway of Staphylococcus aureus. *Journal of bacteriology* **191**, 851-861, doi:10.1128/JB.01357-08 (2009).
28 Swoboda, J. G., Campbell, J., Meredith, T. C. & Walker, S. Wall teichoic acid function, biosynthesis, and inhibition. *Chembiochem : a European journal of chemical biology* **11**, 35-45, doi:10.1002/cbic.200900557 (2010).
29 Del Val, E., Nasser, W., Abaibou, H. & Reverchon, S. RecA and DNA recombination: a review of molecular mechanisms. *Biochemical Society transactions* **47**, 1511-1531, doi:10.1042/BST20190558 (2019).
30 Johnston, C. D. *et al.* Systematic evasion of the restriction-modification barrier in bacteria. *Proceedings of the National Academy of Sciences of the United States of America* **116**, 11454-11459, doi:10.1073/pnas.1820256116 (2019).
31 Papanastasiou, M. *et al.* The Escherichia coli peripheral inner membrane proteome. *Molecular & cellular proteomics : MCP* **12**, 599-610, doi:10.1074/mcp.M112.024711 (2013).
32 Spry, C., Kirk, K. & Saliba, K. J. Coenzyme A biosynthesis: an antimicrobial drug target. *FEMS microbiology reviews* **32**, 56-106, doi:10.1111/j.1574-6976.2007.00093.x (2008).
33 Vestergaard, M. *et al.* Inhibition of the ATP Synthase Eliminates the Intrinsic Resistance of Staphylococcus aureus towards Polymyxins. *mBio* **8**, doi:10.1128/mBio.01114-17 (2017).

34 Nishi, H., Komatsuzawa, H., Fujiwara, T., McCallum, N. & Sugai, M. Reduced content of lysyl-phosphatidylglycerol in the cytoplasmic membrane affects susceptibility to moenomycin, as well as vancomycin, gentamicin, and antimicrobial peptides, in Staphylococcus aureus. *Antimicrobial agents and chemotherapy* **48**, 4800-4807, doi:10.1128/AAC.48.12.4800-4807.2004 (2004).
35 Ruzin, A. *et al.* Inactivation of mprF affects vancomycin susceptibility in Staphylococcus aureus. *Biochimica et biophysica acta* **1621**, 117-121, doi:10.1016/s0304-4165(03)00028-x (2003).
36 Coe, K. A. *et al.* Multi-strain Tn-Seq reveals common daptomycin resistance determinants in Staphylococcus aureus. *PLoS pathogens* **15**, e1007862, doi:10.1371/journal.ppat.1007862 (2019).
37 Slavetinsky, C. J. *et al.* Sensitizing Staphylococcus aureus to antibacterial agents by decoding and blocking the lipid flippase MprF. *eLife* **11**, doi:10.7554/eLife.66376 (2022).
38 Bayer, A. S. *et al.* Transposon disruption of the complex I NADH oxidoreductase gene (snoD) in Staphylococcus aureus is associated with reduced susceptibility to the microbicidal activity of thrombin-induced platelet microbicidal protein 1. *Journal of bacteriology* **188**, 211-222, doi:10.1128/JB.188.1.211-222.2006 (2006).
39 Taber, H. W., Mueller, J. P., Miller, P. F. & Arrow, A. S. Bacterial uptake of aminoglycoside antibiotics. *Microbiological reviews* **51**, 439-457 (1987).
40 Vioque, A. & de la Cruz, J. Trans-translation and protein synthesis inhibitors. *FEMS microbiology letters* **218**, 9-14, doi:10.1111/j.1574-6968.2003.tb11491.x (2003).
41 Cerullo, F. *et al.* Bacterial ribosome collision sensing by a MutS DNA repair ATPase paralogue. *Nature* **603**, 509-514, doi:10.1038/s41586-022-04487-6 (2022).
42 Linder, P., Lemeille, S. & Redder, P. Transcriptome-wide analyses of 5'-ends in RNase J mutants of a gram-positive pathogen reveal a role in RNA maturation, regulation and degradation. *PLoS genetics* **10**, e1004207, doi:10.1371/journal.pgen.1004207 (2014).
43 Dai, L. *et al.* Identification of small-molecule inhibitors of the DNA repair proteins RuvAB from Pseudomonas aeruginosa. *Bioorganic & medicinal chemistry* **73**, 117022, doi:10.1016/j.bmc.2022.117022 (2022).
44 Jin, J. *et al.* Evaluation of small molecule SecA inhibitors against methicillin-resistant Staphylococcus aureus. *Bioorganic & medicinal chemistry* **23**, 7061-7068, doi:10.1016/j.bmc.2015.09.027 (2015).
45 Cacace, E. *et al.* Systematic analysis of drug combinations against Gram-positive bacteria. *Nature microbiology* **8**, 2196-2212, doi:10.1038/s41564-023-01486-9 (2023).
46 Diep, B. A. *et al.* Complete genome sequence of USA300, an epidemic clone of community-acquired meticillin-resistant Staphylococcus aureus. *Lancet* **367**, 731-739, doi:10.1016/S0140-6736(06)68231-7 (2006).
47 Balaban, N. Q. *et al.* Definitions and guidelines for research on antibiotic persistence. *Nature reviews. Microbiology* **17**, 441-448, doi:10.1038/s41579-019-0196-3 (2019).
48 Lobritz, M. A. *et al.* Antibiotic efficacy is linked to bacterial cellular respiration. *Proceedings of the National Academy of Sciences of the United States of America* **112**, 8173-8180, doi:10.1073/pnas.1509743112 (2015).
49 Jawetz, E., Gunnison, J. B. & Coleman, V. R. The Combined Action of Penicillin with Streptomycin or Chloromycetin on Enterococci in Vitro. *Science* **111**, 254-256, doi:10.1126/science.111.2880.254 (1950).
50 Kwan, B. W., Valenta, J. A., Benedik, M. J. & Wood, T. K. Arrested protein synthesis increases persister-like cell formation. *Antimicrobial agents and chemotherapy* **57**, 1468-1473, doi:10.1128/AAC.02135-12 (2013).
51 Ocampo, P. S. *et al.* Antagonism between bacteriostatic and bactericidal antibiotics is prevalent. *Antimicrobial agents and chemotherapy* **58**, 4573-4582, doi:10.1128/AAC.02463-14 (2014).
52 Wang, Y. *et al.* Inactivation of TCA cycle enhances Staphylococcus aureus persister cell formation in stationary phase. *Scientific reports* **8**, 10849, doi:10.1038/s41598-018-29123-0 (2018).

53 Kim, J. S. *et al.* Fumarate-Mediated Persistence of Escherichia coli against Antibiotics. *Antimicrobial agents and chemotherapy* **60**, 2232-2240, doi:10.1128/AAC.01794-15 (2016).
54 Babu, M. *et al.* Quantitative genome-wide genetic interaction screens reveal global epistatic relationships of protein complexes in Escherichia coli. *PLoS genetics* **10**, e1004120, doi:10.1371/journal.pgen.1004120 (2014).
55 Peters, J. M. *et al.* A Comprehensive, CRISPR-based Functional Analysis of Essential Genes in Bacteria. *Cell* **165**, 1493-1506, doi:10.1016/j.cell.2016.05.003 (2016).
56 Bates, D. & Kleckner, N. Chromosome and replisome dynamics in E. coli: loss of sister cohesion triggers global chromosome movement and mediates chromosome segregation. *Cell* **121**, 899-911, doi:10.1016/j.cell.2005.04.013 (2005).
57 Arjes, H. A. *et al.* Failsafe mechanisms couple division and DNA replication in bacteria. *Current biology : CB* **24**, 2149-2155, doi:10.1016/j.cub.2014.07.055 (2014).
58 Lemon, K. P. & Grossman, A. D. The extrusion-capture model for chromosome partitioning in bacteria. *Genes & development* **15**, 2031-2041, doi:10.1101/gad.913301 (2001).
59 Bae, T. *et al.* Staphylococcus aureus virulence genes identified by bursa aurealis mutagenesis and nematode killing. *Proceedings of the National Academy of Sciences of the United States of America* **101**, 12312-12317, doi:10.1073/pnas.0404728101 (2004).
60 Jarick, M. *et al.* The serine/threonine kinase Stk and the phosphatase Stp regulate cell wall synthesis in Staphylococcus aureus. *Scientific reports* **8**, 13693, doi:10.1038/s41598-018-32109-7 (2018).
61 Kaushik, S., He, H. & Dalbey, R. E. Bacterial Signal Peptides- Navigating the Journey of Proteins. *Frontiers in physiology* **13**, 933153, doi:10.3389/fphys.2022.933153 (2022).
62 Lenski, R. E., Rose, M. R., Simpson, S. C. & Tadler, S. C. Long-Term Experimental Evolution in Escherichia-Coli .1. Adaptation and Divergence during 2,000 Generations. *American Naturalist* **138**, 1315-1341, doi:Doi 10.1086/285289 (1991).
63 Wiser, M. J. & Lenski, R. E. A Comparison of Methods to Measure Fitness in Escherichia coli. *PloS one* **10**, e0126210, doi:10.1371/journal.pone.0126210 (2015).
64 Goodarzi, H., Elemento, O. & Tavazoie, S. Revealing global regulatory perturbations across human cancers. *Molecular cell* **36**, 900-911, doi:10.1016/j.molcel.2009.11.016 (2009).

Figure 1. Investigating the genetic landscape of antibiotic sensitivity in Staphylococcus aureus with CALM-CRISPRi

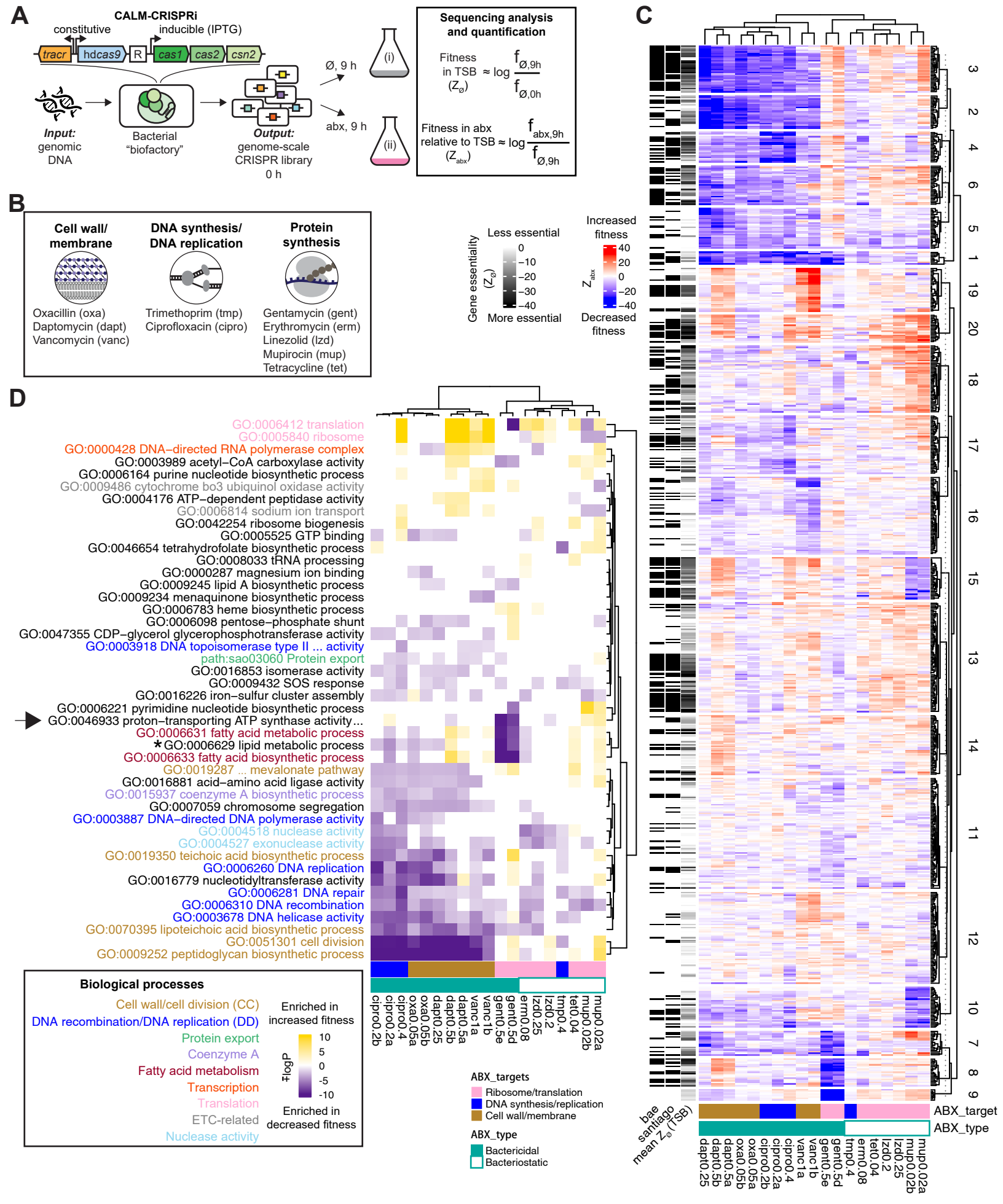

Figure 2. Essential genes dominate antibiotic-gene interactions

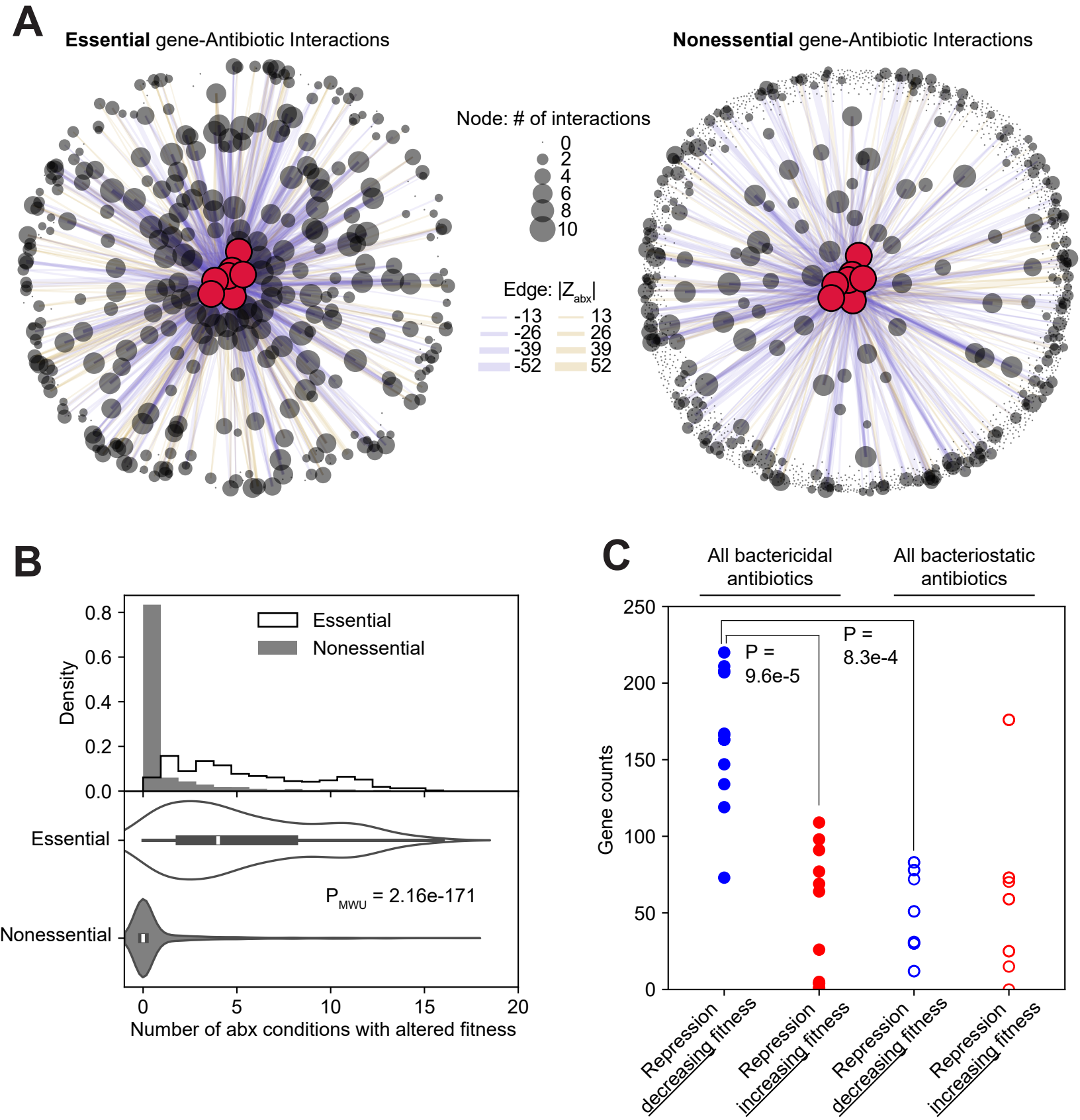

Figure 3. Widespread CCDD synergy

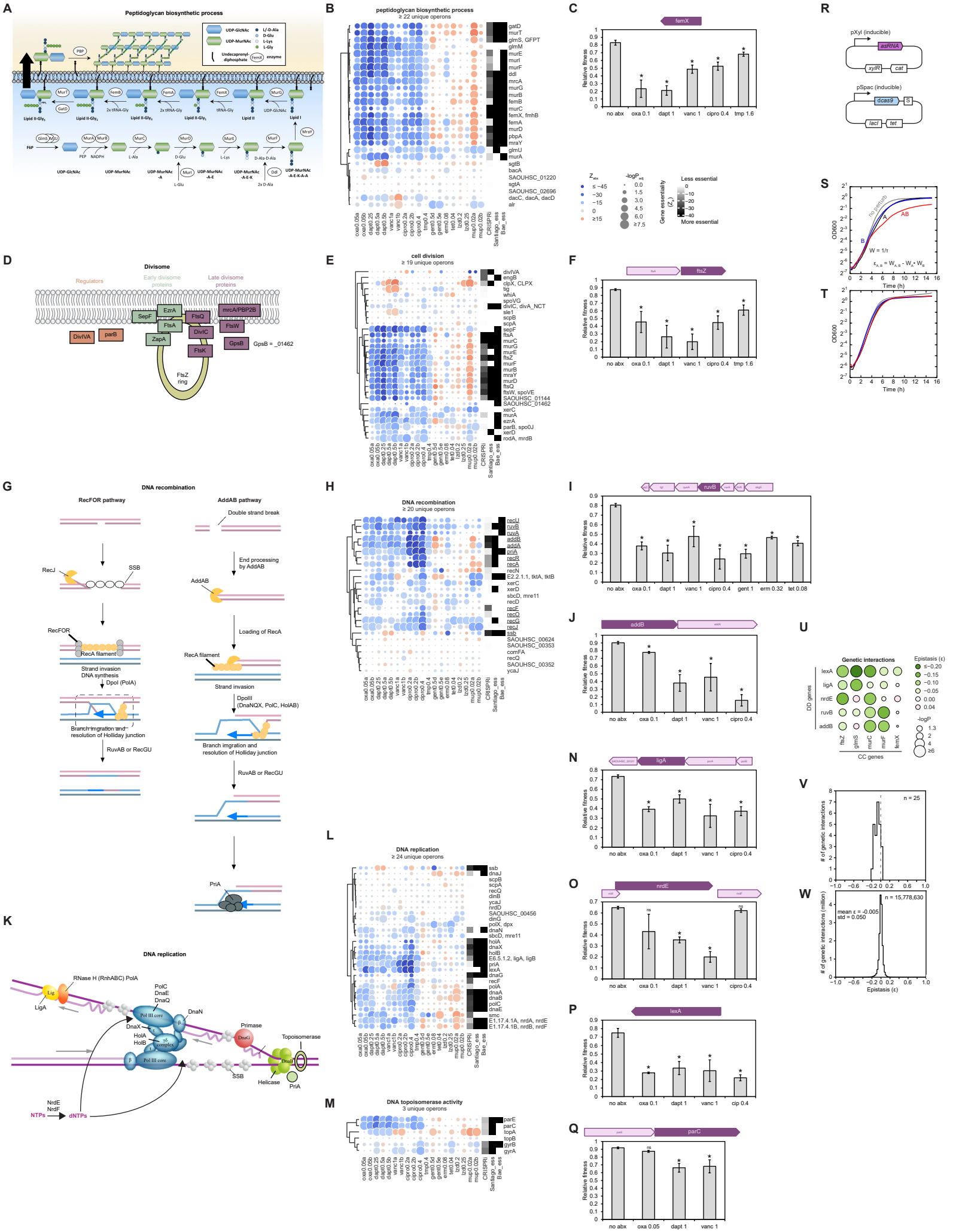

Figure 4. Protein export and cofactor biosynthesis

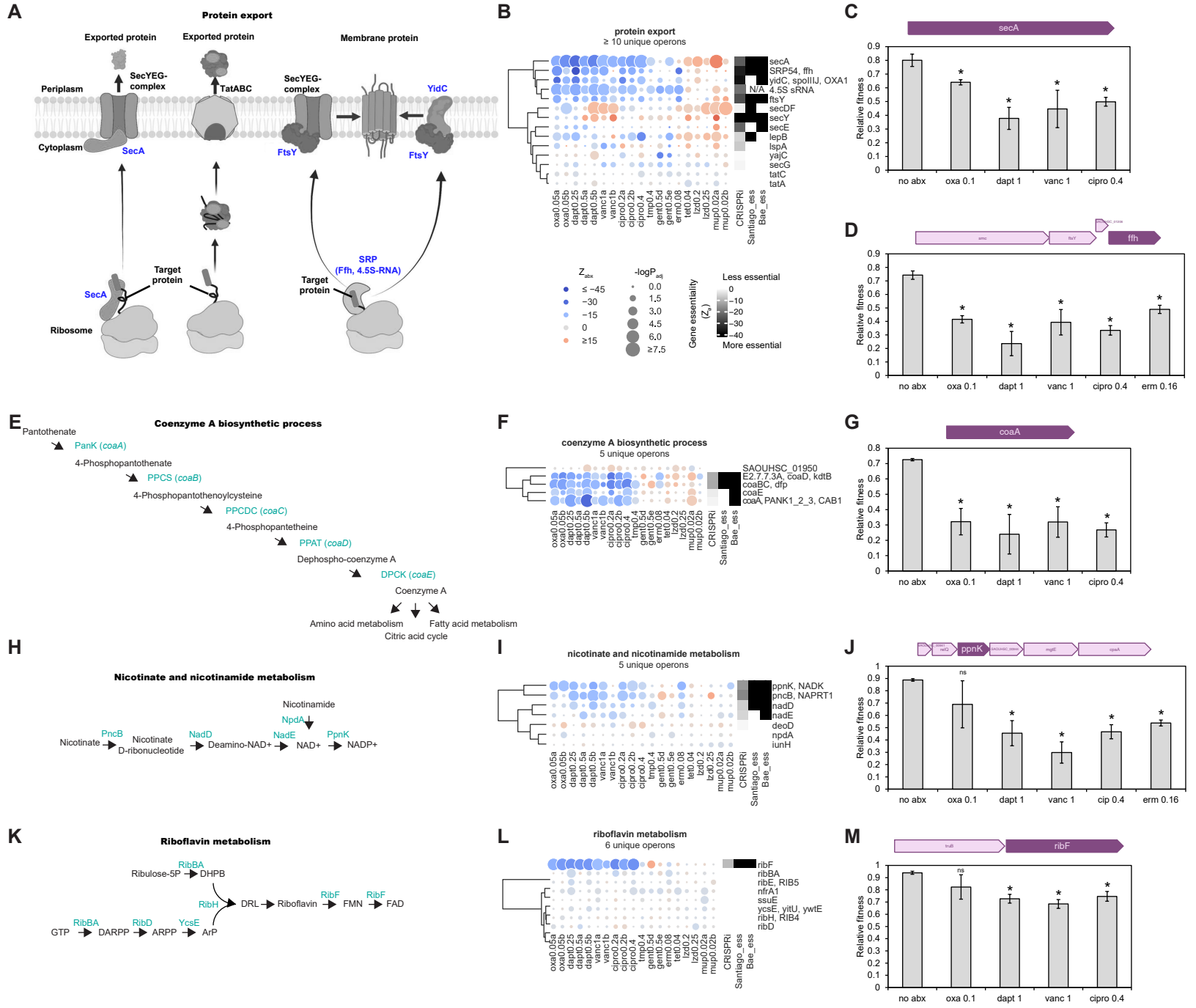

Figure 5. Repression of transcription and translation antagonizes bactericidal antibiotics

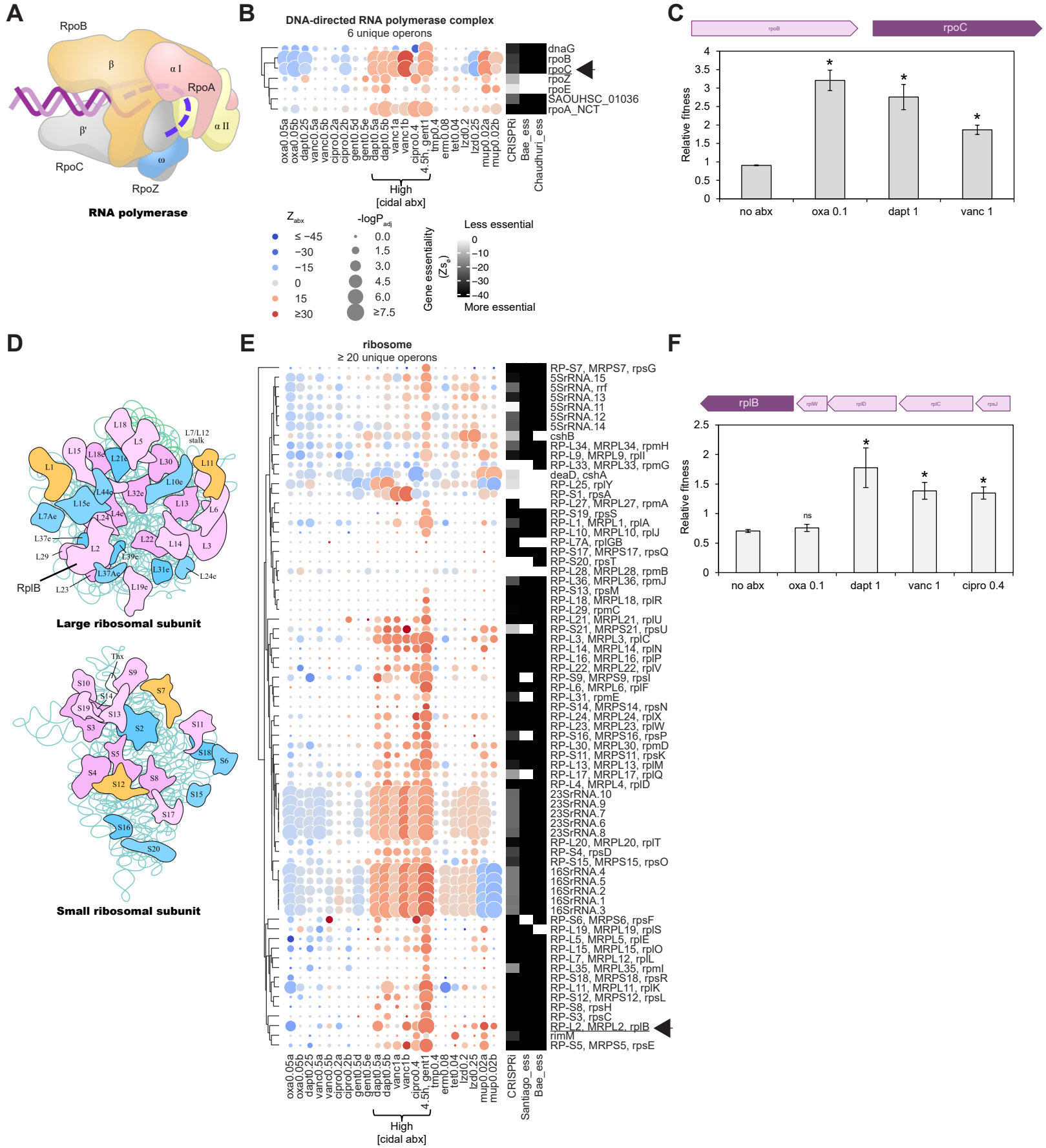

Figure 6. Select nuclease activity affects fitness in bacteriostatic antibiotics

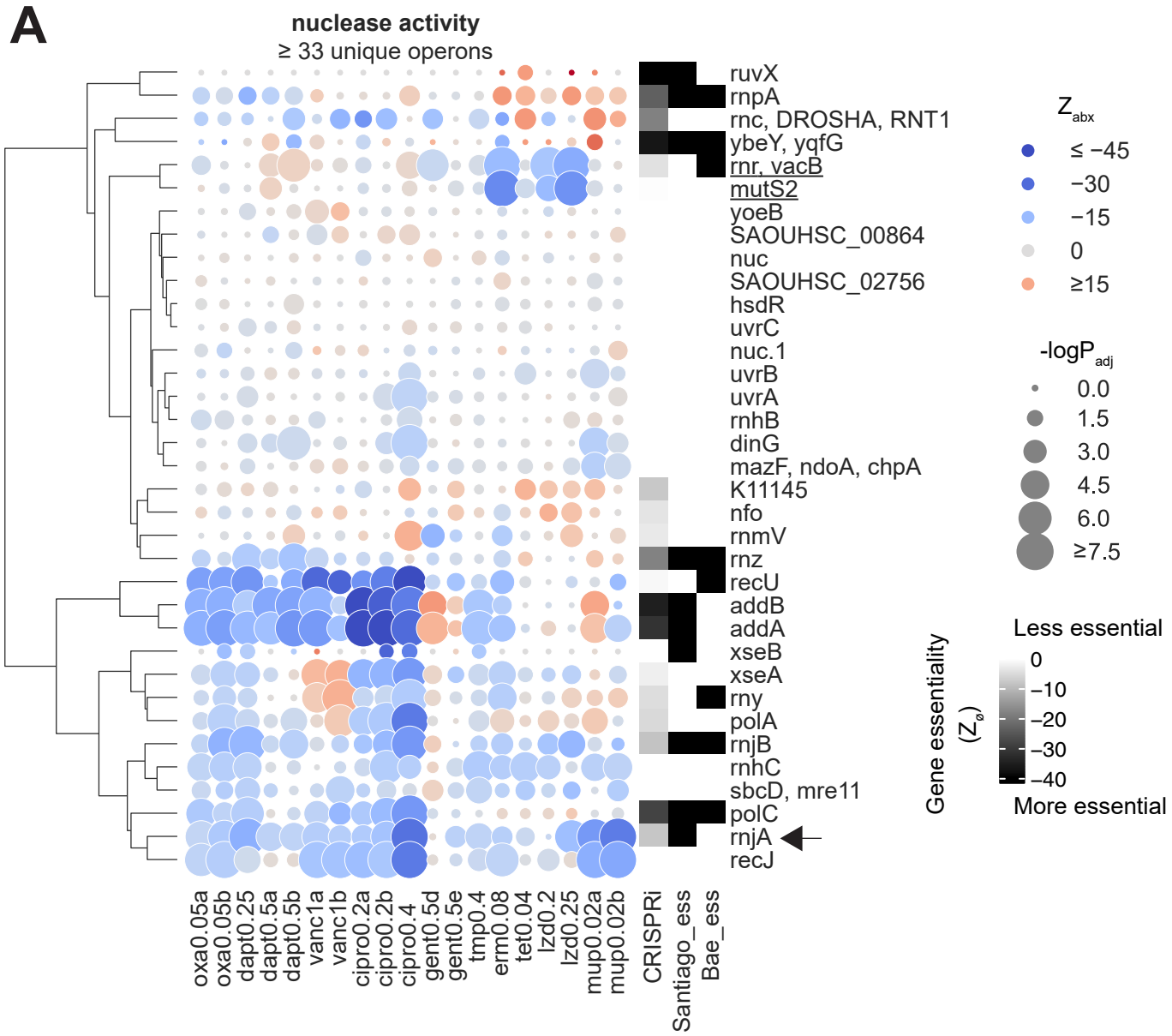

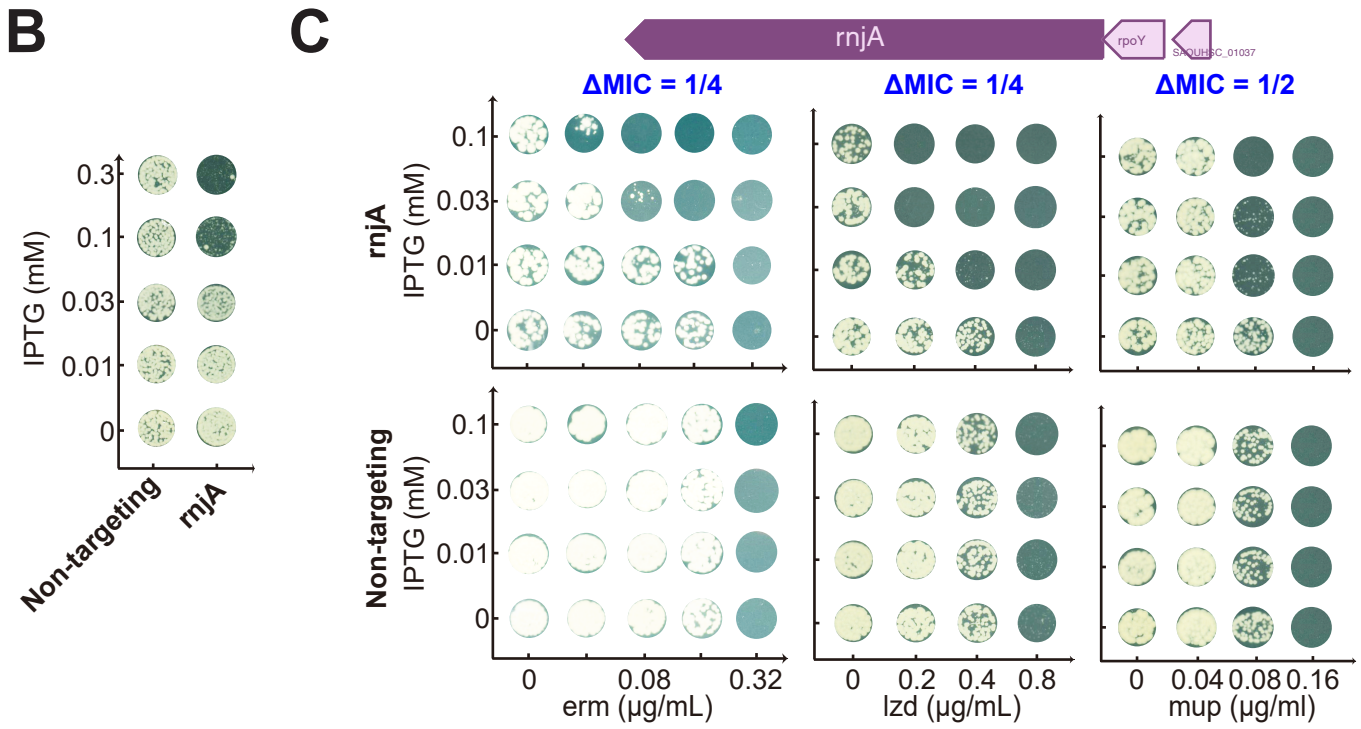
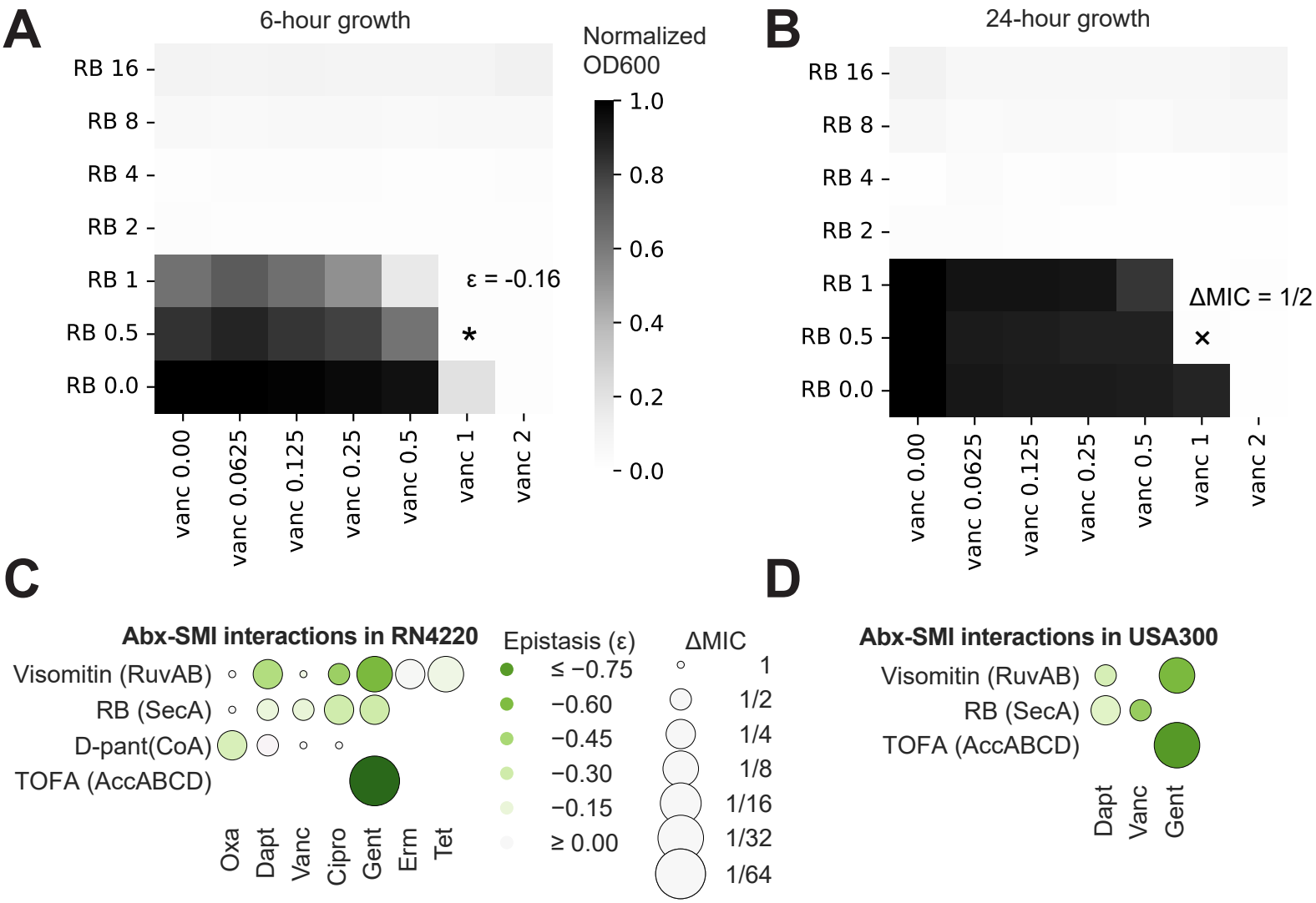
Figure 7. Synergistic drug combinations